A BROAD BAND DOUBLE BALANCED MIXER

by

SQN LDR NIRANJAN SWAIN

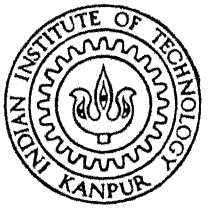

DEPARTMENT OF ELECTRICAL ENGINEERING

INDIAN INSTITUTE OF TECHNOLOGY KANPUR

MARCH, 1990

A BROAD BAND DOUBLE BALANCED MIXER

A Thesis Submitted
in Partial Fulfilment of the Requirements
for the Degree of

MASTER OF TECHNOLOGY

by

SQN LDR NIRANJAN SWAIN

to the

DEPARTMENT OF ELECTRICAL ENGINEERING
INDIAN INSTITUTE OF TECHNOLOGY KANPUR

MARCH, 1990

26/3/90

C E R T I F I C A T E

It is certified that the work contained in the thesis entitled "A Broad Band Double Balanced Mixer" by Sqn Ldr Niranjan Swain, has been carried out under my supervision and that this work has not been submitted elsewhere for a degree .

M Sachidananda

Signature of Supervisor

Name M. Sachidananda .

Department Electrical Engineering .

Indian Institute of Technology , Kanpur .

March, 1990 .

ABSTRACT

This project was started with an aim of designing and fabricating a broad band double balanced mixer using a diode quad. Two different configurations are adopted for the work. The first configuration consists of microstrip feed lines with CPW junction as ring quad driver and slot line as transmission line to launch an even mode in the CPW. The design of various transitions with impedance transformers,Power dividers and uncoupled junctions of microstrip line and slot line are carried out based on data available. However, lack of sufficient data led to formulation of empirical design. The above mixer gave good performance over 2.5 GHz to 4.5 GHz. The diode quad is designed for operation up to 3 GHz and hence the noise figure was found to be high at higher frequencies. If a diode quad designed for 10GHz operation is used in the same circuit it is expected that much better noise performance can be obtained over larger band width. The circuit elements seemed to give larger mismatch losses at higher frequencies. The reason for poorer performance is mainly due to the lack of precision etching. Presence of several transitions from microstrip to slot line ,power dividers etc , give rise some VSWR at each , which combine to deteriorate the mixer performance.

The second configuration to improve upon the first one was adopted in which some of the previous draw backs are eliminated. This configuration consists of driving a quad by symmetrical

double strip transmission line kept physically orthogonal to achieve isolation between LO and RF signals. This configuration also uses transition from microstrip to double strip transmission line with impedance transformation. The design details of transition from a microstrip to double strip line is not available in literature. Therefore, an empirical formula is derived for the transition region where the lines has two strips of different width. The performance of the mixer is found to be better from 2GHz to 6.5GHz. However, the mismatches in the circuit at some frequency is found to be high. This may be due to resonances at these frequencies. The conversion loss is within 6 dB from 2 GHz to 5 GHz. The measured noise figure is below 5dB from 2GHz to 3GHz The noise figure is within 10 dB from 3GHz to 5GHz. The second configuration is found to have better performance than the first configuration.

ACKNOWLEDGEMENT

I very gratefully acknowledge my thesis supervisor Dr.M.Sachidananda, who initiated me into the work reported in this thesis and provided with in valuable and unfailing guidance for carrying out this work.

I am indebted to my colleague Mr.Jaideva.C.Goswami for his helps and cheerful company through out my stay here. I am thankful to Mr.V. Seethram for his help during the thesis preparation.

I am thankful to Mr.S.K. Kole of PCB Lab and Mr.P.H.Tiwari of Electrical Workshop for their sincere help at every stage of this project.

Last but not the least a special word of thanks to my wife, Priya, for being a source of inspiration.

In loving memory of my brothers

Er. S. B. Swain

and

Dr. T. N. Swain

CONTENTS

CHAPTER 1

INTRODUCTION

1.1 INTRODUCTION

The basic principles of frequency conversion using crystal diodes were first studied in depth by Torrey and Whitmer [1] in 1948. Microwave diode mixers have been used for many years to obtain conversion of a signal at microwave frequencies to one at a much lower frequency. Such mixers have been the subject of much study and development. However, there is a continuing need for improvements which can result in better electrical performance, higher reliability, improved reproducibility and lower production cost.

There have been well known techniques for the enhancement of mixer operation by the proper control of the impedances at each of the mixer terminals and at each of frequencies of importance. The frequencies of importance are modulation products which exist according to the heterodyne principle by which the mixer operates. The received signal (RF), together with a higher level of signal from a local oscillator (LO), are applied to a non linear element. The RF is mixed with the LO producing the sum frequency LO + RF, the difference (or intermediate) frequency (IF), LO - RF, and the image frequency 2LO - RF.

Microwave Integrated Circuits (MIC) balanced mixers have been produced for use in high frequency bands [2]...[5]. Balanced type mixers have several desirable features, such as good isolation and suppression of undesired signals. MIC balanced mixers have been constructed using combination of microstrip lines, slot lines and coplanar lines. But, most commonly used mixers at higher frequencies are double balanced mixers. Their advantages over the single balanced are inherent isolation between all ports without filters, spurious response rejection, LO noise suppressions, lower intermodulation and extremely broad band operation. They have the disadvantage of using four diodes at least with two hybrids. They have greater LO power requirements and generally have higher conversion loss.

Broad band double balanced mixer can be produced by several configurations in MIC. However, due to the complexity of the circuit configuration the double balanced mixers are not easily fabricated. The aim in this project work is design and fabrication of MIC double balanced circuits for a broad band operation. Two configuration in MIC designs have been tried, The performance characteristics of both the circuits have been studied. The circuits adopted for the work is less frequency sensitive. In the process of mixer design several transitions between slot line and microstrip line were studied and were characterized experimentally. Different types of near-isolated slot line and microstrip junctions were characterized. The best suited transitions and uncoupled junction designs have been adopted in the present work. The first configuration for the

double balanced mixer is designed with a combination of microstrip lines, slot lines and coplanarwaveguide(CPW). The second configuration is designed with microstrip line and symmetrical double strip transmission lines [6].

1.2 LITERATURE SURVEY

The microwave mixer for operation at X-band on an integrated mixer circuit having low conversion loss have been reported by Dickens [2]. The measured conversion loss was under 3.15 dB. The intermodulation in diode ring mixers due to non linearity of diode switches and due to interference by signal voltages with LO switching function have been reported by HP Walker [11]. GaAs schottky barrier diodes with a zero-bias cut-off frequency of 800 GHz have been used in an integrated circuit balanced diode mixer operating with a signal frequency centered at 9.3 GHz and LO frequency at 7.8 GHz by Dickens[2]. A novel thin film down converter which is pumped at a sub multiple of the LO frequency has given a conversion loss which is comparable to the performance of conventional balanced mixers as reported by Schneider [4]. Hiroyo Ogawa,et al.[5] have reported a novel microwave integrated double balanced mixer with good isolation between the three ports. That mixer was fabricated using a combination of microstrip lines, slot lines and coupled slot lines, together with four beam-lead schottky-barrier diodes. the analysis and design of microwave balanced mixers have been reported by Bernd Schuppert [12]. He has also investigated the effect of circuit and diode parameters and various performances of

the mixer.

Various designs like a transmission line taper of improved design as reported by RW Klopfenstein [13] have been surveyed. The improved microstrip to microslot transitions has been reported by B.Schiek et al.[8].

1.3 ORGANIZATION OF THE THESIS

The analysis of a double balanced mixer with its equivalent circuit has been the matter of discussion of chapter two. The important mixer parameters and performance indices have been included. The mixer design consideration for the present work are also elaborated.

Design consideration and the double balanced mixer configuration arrived at the present work has been presented in chapter three. Different components such as, transitions, junctions between microstrip and slot lines and CPW have also been analyzed.

The fabrication work and design details have been reported in chapter four. The ring quad specifications and the different performance characteristics of double balanced mixer with measurement set-ups have also been dealt with. Different performance characteristic graphs are included.

The performance characteristics of the CPW junction double balanced mixer was not up to the expectation due to various

reasons. This has been discussed in the chapter four. Another configuration with microstrip to balanced double strip transmission line has been fabricated. The details of this circuit including performance characteristics are discussed in chapter 5.

Chapter six recapitulates the total work and the future scope for this work.

CHAPTER 2

ANALYSIS OF DOUBLE BALANCED MIXER

2.1 INTRODUCTION

The primary purpose of a mixer is to translate a signal at one frequency to another,where it can be amplified or processed properly and more effectively. To achieve the desired function with minimal added noise or distortion is more important. An ideal mixer is the one which simply multiplies the radio frequency (RF) and Local Oscillator (LO)signals.

Let the RF input be

$$V_1(t)=A_1 \sin \omega_s t \qquad 2.1$$

Let the LO input be

$$V_2(t)=A_2 \sin \omega_1 t \qquad 2.2$$

Where ω_s and ω_1 are rotational frequency of RF and LO respectively.

Then the output can be represented by V_0,given by,

$$V_0(t)= A_1 \sin \omega_s t(A_2 \sin \omega_1 t)$$

$$= \frac{A_1 A_2}{2} \quad [\cos (\omega_s-\omega_1)t - \cos (\omega_s+\omega_1)t] \qquad 2.3$$

In a common mixer application of down conversion,the difference frequency term $(\omega_s-\omega_1)$ is the desired IF output. The sum frequency $(\omega_s+\omega_1)$ is rejected using low pass filter. In a broad band circuit harmonics of the LO i.e. $2\omega_1, 3\omega_1$...etc are generated by the nonlinearity action.Different harmonics generated have

power level of $\frac{1}{n^2}$,where n is the 'n' th harmonic. The RF signal is mixed with $\omega_1, 2\omega_1$ etc producing the sum i.e. $\omega_s+\omega_1$ and difference frequency of $\omega_s-\omega_1$ or ω_{IF}. ω_{IF} is known as Intermediate frequency. There is an Image frequency , which is the mirror image of the signal with respect to the LO frequency.

If image frequency is represented by ω_I, then

$$\omega_I=2\omega_1-\omega_s \qquad 2.4$$

For a very broad band circuit a nonlinear resistor is equally efficient in producing the sum and difference frequencies. The spectrum after first mixing process is shown in fig.2.1. Since the mixer is assumed to be matched to the IF amplifier, the power at ω_{IF} will be transmitted to IF amplifier. Both, the new side bands ω_I and sum frequency will tend to propagate out of the mixer and into the microwave circuit.

Mixers are classified as

(a) Single ended mixer

(b) Balanced mixer

(1) Single balanced mixer

(2) Double balanced mixer

(a) Single Ended Mixer :

All the types of mixers using a single diode are described as single ended mixer. They are basic to the design of all

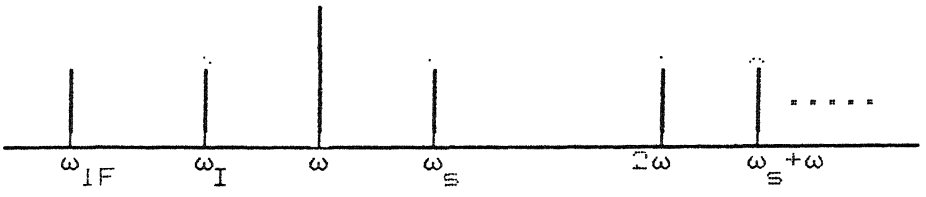

$\omega_{IF} = \omega_s - \omega$: Intermediate frequency

$\omega_{sum} = \omega_s + \omega$: Sum frequency

$\omega_I = 2\omega - \omega_s$: Image frequency

$\omega_{IF} = \omega - \omega_I = \omega_{sum} - 2\omega$

Fig 2.1. First and second order modulation products .

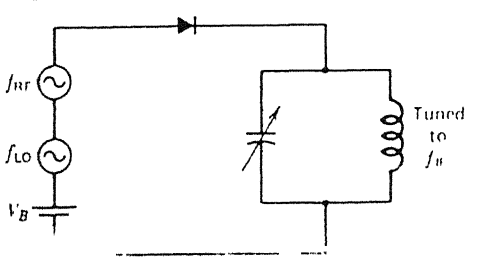

Fig 2.2. A simple diode mixer circuit .

mixers, especially balanced or multi-diode configuration. Fig 2.2 shows a simple single ended mixer. The single diode is placed in series with RF and LO inputs with a bias source. The circuit has high noise figure and less isolation between LO and RF .

(b) Balanced Mixer :

Balanced mixers overcome the disadvantage of the single ended type and have additional advantages. Balanced mixers generally have better power handling capability. They also reject the LO noise effectively. It has the disadvantage of poorer conversion performance. There are two types of balanced mixers.

(1) single balanced mixer circuits

(2) double balanced mixer circuits

(1) Single Balanced Mixer Circuits :

This utilizes two non-linear devices with RF and LO inputs applied in push pull fashion so that the frequency component and its odd harmonics do not appear in the IF port.

(2) Double Balanced Mixer Circuits :

This utilizes four non-linear devices. It has both the RF and LO inputs to separate ports in push pull fashion so that neither signal appear at the two other ports i.e.the LO signal does not appear at the RF port or at the IF port and so forth. These circuits generally require well balanced input and out put transformers and accurate matching of the active device characteristics. The details of the double balanced circuits

will be discussed in the next section.

2.2 DOUBLE BALANCED MIXER OPERATION

(a) Configuration :

Double balanced mixer can be achieved by using a ring or a cross configuration of diodes. The mixer operation can be described qualitatively by treating diodes as switches. The switches are operated by LO voltages. This approach assumes that the conductance waveform of a diode is a square wave. This assumption is valid as long as the LO level is large enough to make the diode conduct fully. Fig 2.3 shows double balanced mixer equivalent circuit. Four diodes are arranged in the double balanced configuration. The RF signal is applied to the RF port primary winding. The LO signal is applied to the primary of the LO port transformer primary. The output is generally tapped from center point of each transformer.

(b) Operation :

(i) On positive half cycle of LO :

When LO signal is applied to the nodes c and d with c as positive and d as negative , then diodes D1 and D2 will conduct. During this time the diodes D3 and D4 will be reverse biased. If the junction and series resistance of the forward biased diodes are low then they can be approximated as closed switches. The currents at the RF frequency i.e., i_1 and i_2 flow in the diodes when point a is positive with respect to e and b The LO current will flow around the loop as c-a-d-f-c. The currents i_1 and i_2 are due to the voltage across a to e . These currents produce a

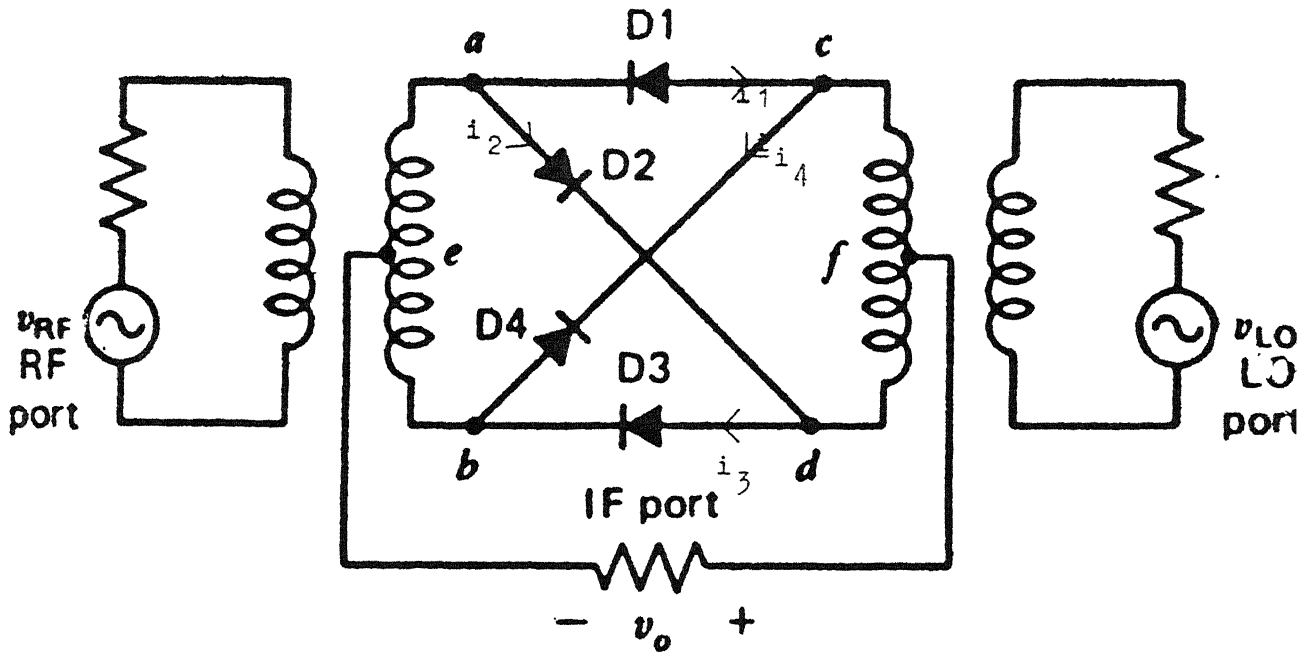

R_s :Source resistance

R_L :LO resistance

V_{RF}:RF voltage

V_{LO}:LO voltage

Fig 2.3. Double balanced equivalent circuit.

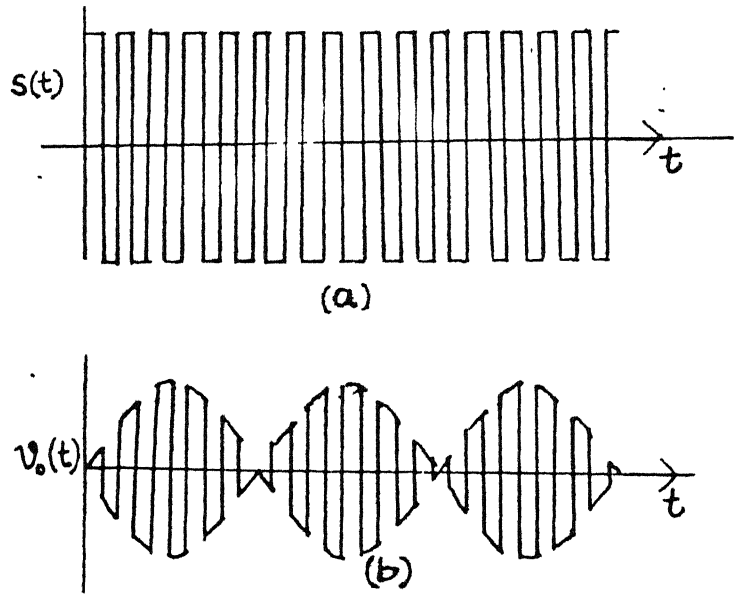

Fig 2.4(a). Switching function of the mixer.

Fig 2.4(b). Output voltage waveform in Resistive Load.

voltage V_o with polarity as shown in the fig.2.4. Here the LO current does not flow in the RF transformer winding. Also the point a and f are at same potential (at ω_1),if the diodes are perfectly balanced.

(ii) On negative half cycle of LO :

During the negative half cycle of LO the point 'c' is negative and 'd' is positive. This forces the diodes D4 and D3 to conduct and D1 and D2 to cutoff. At this time the RF voltage V_{eb} produces the current i_3 and i_4 as indicated in fig 2.3.The sum of these currents flow in the load from left to right producing V_o of opposite polarity to the previous half cycle of LO. Here also the LO current does not flow in the RF transformer. Therefore the RF port is isolated from the LO port.

Also in both cases the RF currents flowing in the opposite directions in the two halves of the LO windings so that no voltage of frequency f_{RF} is induced in LO port if the LO transformer is exactly center tapped.

The switching function produced by V_1 and the diodes are as shown in fig 2.4(a) and is expressed mathematically as :

$$S(t)= 2 \sum_{n=1}^{\infty} \frac{\sin n\pi/2}{n\pi/2} \cos n\omega_1 t \qquad 2.5$$

Where ω_1 is the LO frequency , t is the time .

If RF voltage is represented by $V_{RF} \cos \omega_{RF} t$, where ω_{RF} is RF frequency ,t is the time, then output can be expressed as:

$$V_0(t)=2\ V_{RF}\cos\omega_{RF}t\ \left(\sum_{n=1}^{\infty}\frac{\sin n\pi/2}{n\pi/2}\cos n\omega_1 t\right) \qquad 2.6$$

Therefore the output spectrum will have only frequencies $nf_1 \pm f_{RF}$, with n as odd. Neither f_1 nor f_{RF} appears at the output. This is shown in fig 2.4(b).

2.3 MIXER PARAMETERS

A mixer is characterized by the following parameters.

(i) Conversion Loss

(ii) noise figure

(iii) Third order intercept point

(iv) port to port isolation

(v) conversion compression

(i) Conversion Loss: It is one of the most important mixer parameter, specially for receiver input stages. This is defined as the ratio of output power in one side band to signal input power.

$$L=\frac{\text{Available output IF power}}{\text{Available input signal power}}$$

This definition of conversion loss is dependant on the load at the signal port. So L is a function of both the circuit and the intrinsic properties of the non linear device.

(ii) Noise figure: The dominant noise sources in schottky-barrier diodes are thermal noise generated in the series resistance and

shot noise arising from carrier emission across the junction. These are , in almost all the cases, overwhelmingly the dominant noise sources in diode mixers. Other effects such as hot electron noise and intervally scattering noise in GaAs, may dominate in poorly designed or poorly fabricated diodes , or at very high frequencies. The noise analysis which follows will be concerned exclusively with shot and thermal noise.These alone are adequate to give an accurate description of noise behavior in diode mixers.

The most important point in noise analysis is to appreciate the more subtle correlation properties of the noise , and the effect of the time varying elements , particularly the junction capacitance upon them. For the dc- biased diode , the correlation properties are simply those of any white noise process ; components at different frequencies are not correlated. For pumped diodes , however, the components down converted to the IF from different mixing frequencies including unwanted mixing products - are partially correlated , and their correlation raises the noise level.

Shot noise is generated by the diode because , even when biased with dc only , the diode conducts in pulses of current as each electron is emitted across the junction. If the transit time is very short , as it is in schottky-barrier diodes , the current waveform can be treated as a series of random impulses, each of which occurs as a single electron transits the juncton. The average number of such pulses in each second is constant, and is

proportional to the dc current. The instantaneous current varies with time,however, because of the random occurrence of the impulses. Fluctuations in the diode current which result are a noise random process, with a mean squared magnitude proportional to the dc current. The mean squared shot noise current in a forward biased diode is represented as:

$$\bar{i}_s^2 = 2\, qI_j B$$

Where q is the electron charge , I_j is the junction current and B is the band width. An assumption in the above equation is that the electron transit time across the junction is short compared to the inverse of the frequency at which the noise is evaluated.

The other noise source of interest is the thermal noise in the series resistance. The thermal noise is present in any power dissipative medium with a temperature above absolute zero. It arises from the random agitation of electrons , and is closely related to black body radiation. Thermal noise is frequency dependent. However, at low frequencies and high temperature, the noise power available from the resistor depends upon band width and temperature, and not frequency. A resistor of resistance R behaves as if it were noiseless and has a noise voltage source in series with it of magnitude :

$$\bar{V}^2 = 4\ KTBR$$

Therefore the available noise power in a band width B is simply :

$$P_n = KTB$$

Where K is the Boltzmann's constant,T is the absolute temperature in Kelvin. The diode noise equivalent circuit thermal and shot

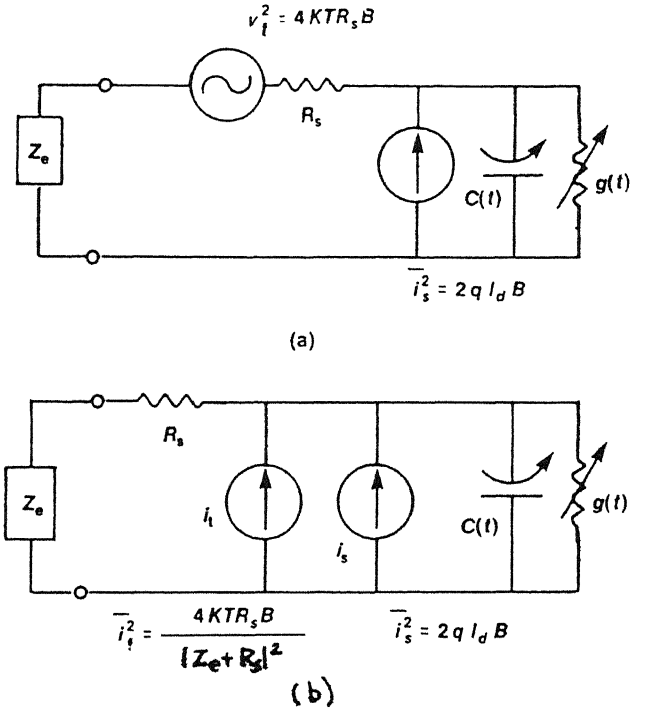

Fig 2.6. Noise equivalent circuit of the diode.

(a) Thermal noise in R_s treated as a voltage source.

(b) Thermal noise source converted to a current source.

noise is represented in fig2.5(a). The thermal voltage source can be converted to a current source via thevnin's theorem , as shown in fig 2.5(b). This representation is more practical for noise analysis.

(iii) Third order intercept point : When two RF signals f_{s1} and f_{s2} are present at the input , an IF given by $(2f_{s2}-f_{s1})\pm f_1$ can be generated by the third order term. The theoretical line relating the input to the output has a slope of 3 , compared to the slope of 1 for the fundamental line. The input level of second RF signal is assumed equal to that of the first. The third order intercept point is where the fundamental line and third order line intercept. The higher the intercept point , the better is the third order suppression. The input frequency and terminating impedances must be specified together with the third order intercept.

(iv) Isolation : This represents the amount of leakage or feed through between mixer ports. Let f_{RF} be the frequency at RF port, f_1 be frequency at LO port and f_{IF} is the IF frequency. Then the f_1 at RF port isolation is the amount ,the f_1 drive level signal is attenuated when measured at the RF port. The f_1 at IF port isolation is the amount the f_1 drive signal is attenuated when measured at the IF port.

(v) Conversion compression : It relates to the RF input power level above which the curves of the IF output power vs RF input power deviates from linearity. Above this level , additional increase in RF input level do not result in proportional increase in output level. Quantitatively, the conversion compression is the output level reduction in dB below the linear characteristic.

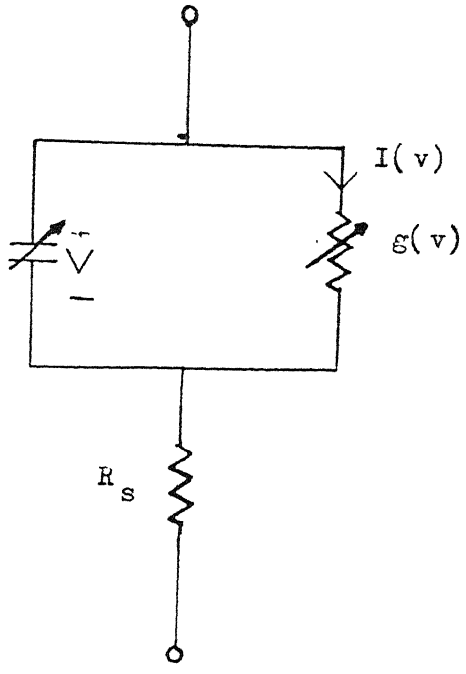

Fig 2.6. Equivalent circuit of a chip diode .

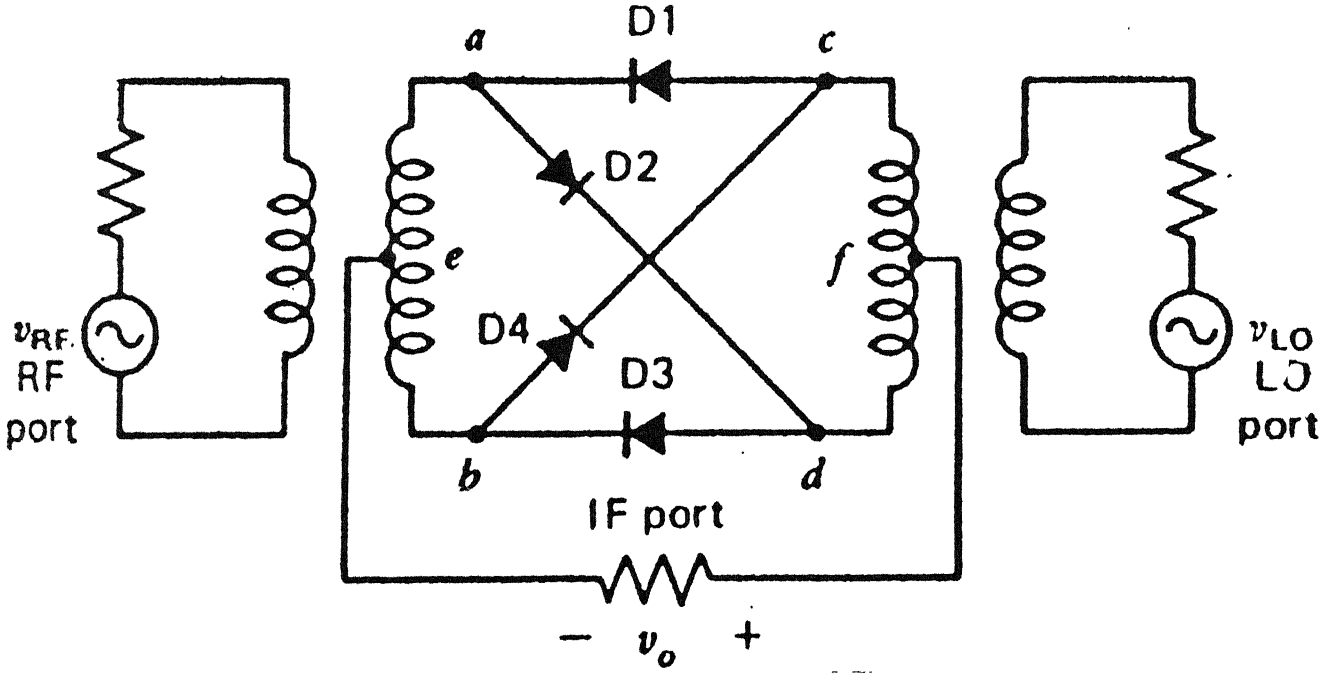

Fig 2.7. Equivalent circuit of a double balanced circuit .

2.4 DIODE CIRCUIT MODEL

The schottky diode is largely immune to minority carrier effect, the junction capacitance and currents are described by

$$C(v) = \frac{C_{jo}}{(1-V/\phi_{bi})^{1/2}} \qquad 2.7$$

where, C_{jo} is the junction capacitance at zero bias voltage

ϕ_{bi} is the built in potential of junction

$$I(v) = I_o[\exp(qv/nKT) - 1] \qquad 2.8$$

where, K is the Boltzmann constant

T is the absolute temperature

n is the ideality factor usually close to 1.

From the above expression it is seen that the junction capacitance and current change instantly with the junction voltage.

A circuit model for the Schottky diode is shown in fig. 2.6. It consists of a voltage variable resistance and capacitance for the junction and fixed series resistance when modeling an actual packaged diode. Other elements have to be added to describe package capacitance and inductance. Generally, the series resistance is assumed to be fixed due to its minor voltage dependence under forward conduction. The control voltage for the capacitance and the junction current is the junction voltage, not the applied voltage, i.e.it must not include the voltage drop

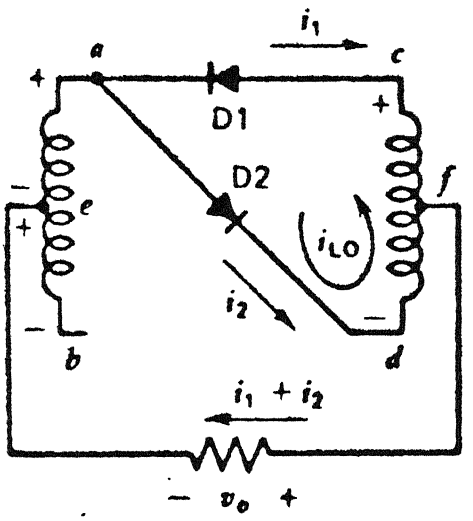

Fig 2.8.Circuit diagram of DBM in positive half cycle of LO.

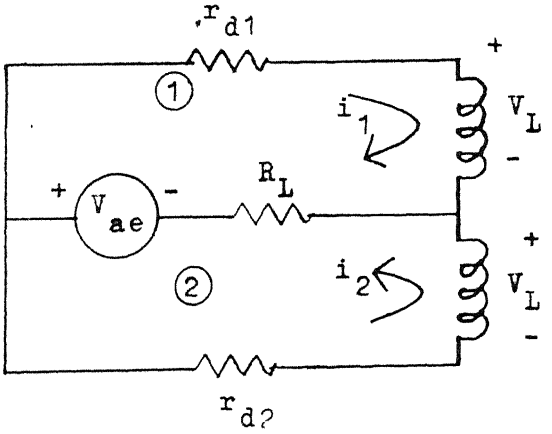

Fig 2.9. DBM equivalent circuit under positive half cycle of LO .

across the series resistance.

2.5 ANALYSIS OF DOUBLE BALANCED MIXER

The equivalent circuit of a Double balanced mixer has been shown in fig. 2.7 . The functioning of this equivalent circuit have been dealt in section 2.2.

When the local oscillator signal is positive the diodes D_1 and D_2 conduct . The equivalent circuit under the positive half cycle of LO is shown in fig. 2.8(a). In the figure i_1 and i_2 are the RF frequency currents in diode D_1 and D_2 respectively. The local oscillator current i_{lo} circulates in the loop c-a-d-f-c and currents i_1 and i_2 combine together to flow in the load resistance. With r_{d1} and r_{d2} as the diode resistances the circuit can be redrawn as shown in fig. 2.9. In this fig R_L is the load resistance, V_L is the LO voltage. V_{ae} is the voltage drop across a-e portion in the secondary of the RF transformer. The RF currents in diodes D_1 and D_2 are i_1 and i_2 respectively.

By applying Kirchoff's voltage law in the loop 1 and loop 2

$$V_{ae} = (i_1+i_2)R_L + i_1 r_{d1} + V_L \qquad 2.9$$

$$V_{ae} = (i_1+i_2)R_L + i_2 r_{d2} - V_L \qquad 2.10$$

On simplification the above equations reduce to

$$2V_{ae} = 2(i_1+i_2)R_L + i_1 r_{d1} + i_2 r_{d2} \qquad 2.11$$

If the diodes characteristics are similar then,

$$r_{d1}=r_{d2}=r_d$$

Therefore,

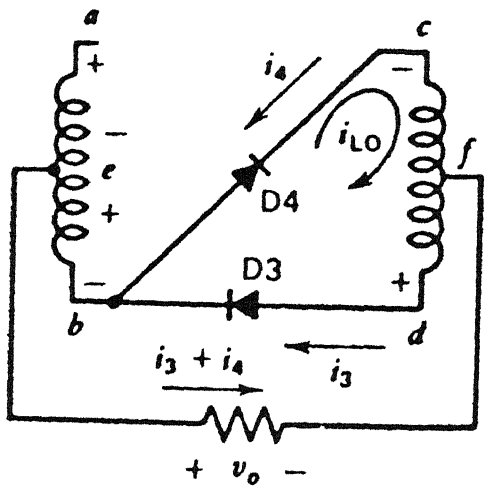

Fig 2.10. circuit diagram of DBM in negative half cycle of LO.

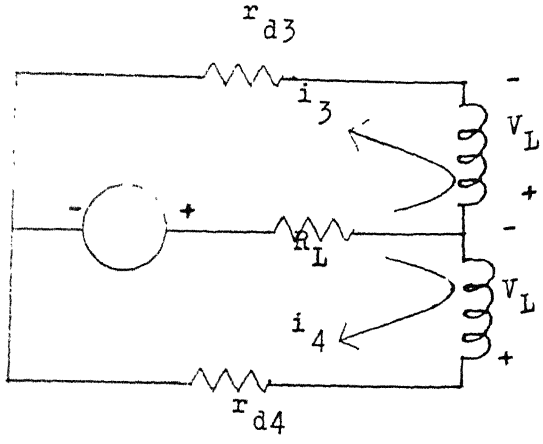

Fig 2.11.DBM equivalent circuit in negative half cycle of LO.

$$2V_{ae} = 2(i_1+i_2)R_L+(i_1+i_2)r_d \qquad 2.12$$

The output voltage V_o is now expressed as

$$V_o = -(i_1+i_2)R_L \qquad 2.13$$

Therefore,

$$\frac{V_o}{V_{ae}} = -\frac{R_L}{R_L+\frac{r_d}{2}} \qquad 2.14$$

But, V_{ae} is the input RF voltage V_{in}

$$\frac{V_o}{V_{in}} = -\frac{R_L}{R_L+\frac{r_d}{2}} \qquad 2.15$$

In a similar manner with LO signal in negative half cycle the equivalent circuit diagram can be drawn as shown in fig. 2.10. Here during negative LO cycle diodes D_4 and D_3 conduct . The RF current i_3 and i_4 flows on the load resistance to produce V_o. During this time diodes D_1 and D_2 are reverse biased. The RF voltage applied is V_{eb}. The forward resistances of diode D_3 and D_4 are represented as r_{d3} and r_{d4}. The equivalent circuit is drawn as shown in fig. 2.11.

On application of Kirchoff's voltage equation to these loops and on simplification

$$\frac{V_0}{V_{in}} = \frac{R_L}{R_L+\frac{r_d}{2}} \qquad 2.16$$

So, in the mixer, the output voltage is proportional to the input voltage and is switched at LO frequency. This can be

expressed as :

$$V_o(t) = V_{in}(p_t) \frac{R_L}{R_L + \frac{r_d}{2}} \qquad 2.17$$

If p_t is a square wave with a frequency equal to that of the LO frequency with DC value no longer equal to zero. p_t can be expressed in a fourier series as:

$$p_t = \frac{2}{\pi} \sum_{n=0}^{\infty} \frac{\sin(2n+1)\omega_1 t}{2n+1} \qquad 2.18$$

Assuming $V_{in}(t)$ as a sine wave and representing it by

$$V_{in}(t) = V_{RF} \sin \omega_{RF} t$$

$$\text{Then } V_o(t) = \frac{R_L}{R_L + \frac{r_d}{2}} \left[\cos \frac{\left[(2n+1)\omega_1 - \omega_{RF}\right]t - \cos\left[(2n+1)\omega_1 + \omega_{RF}\right]t}{2n+1} \right] \qquad 2.19$$

Conversion loss:

$$\text{Mixer conversion loss} = \frac{\text{output power in one sideband}}{\text{input power in one sideband}}$$

Considering the double balanced mixer as shown in fig. 2.3 and equivalent circuit as shown in fig. 2.9 the load impedance as seen by v_i :

$$\frac{v_i}{i_1+i_2} = R_L + \frac{r_d}{2} \qquad 2.20$$

Normally $R_L >> r_d$. So, the input will be matched for maximum power transfer if $R_L = R_s$. Under this condition $V_i = V_{RF}/2$ and input power $= V_{RF}^2/4R_L$.

Output voltage in one side band assuming $R_L >> r_d$ from eqn 2.19

$$V_o\Big|_{\omega_L \pm \omega_i} = \frac{V_{RF}^2}{\pi^2 R_L} \qquad 2.21$$

Therefore,

$$\text{conversion loss} = \frac{V_{RF}^2}{\pi^2 R_L} \times \frac{4R_L}{V_{RF}^2} \qquad 2.22$$

Noise Figure :

Noise Figure =

$$\frac{\text{(available i/p signal power)/(available i/p noise power)}}{\text{(available o/p signal power)/(available o/p noise power)}}$$

This can be represented by :

$$F = \frac{S_{ia} / N_{ia}}{S_{oa} / N_{oa}} = \frac{1}{G_a} \times \frac{N_{oa}}{N_{ia}} \qquad 2.23$$

Where G_a is represented as Available power gain of the mixer.

N_{oa} is Available output noise power $= KT_1B$.

N_{ia} is Available input noise power = KT_0B .

K is Boltzman Constant.

B is the effective Bandwidth.

T_1 is Noise temperature of the output resistance of the network.

T_0 is the Standard noise temperature:290 degree kelvin.

2.6 MIXER DESIGN CONSIDERATIONS

Broad band microwave double balanced mixer can be realized using a ring quad connected properly in a microwave integrated circuit. The main consideration in a Double balanced mixer design are :

(a)Broad band characteristics

(b)Low conversion loss

(c)Low noise figure

However, some aspects are to be considered while designing a double balanced mixer such as :

(d)Spurious response rejection

Double balanced mixer circuits have a property that they are capable of supplying rejection to certain spurious responses associated with the second harmonics of the LO or RF. This is important criteria in the design of a double balanced mixer circuit.

(e)Port VSWR

Port VSWRs are most important criteria in the design of an double balanced mixer. It depends strongly on discontinuities in the connection to the input and output connectors. Poor Port VSWRs will reduce mixer's passband. Therefore, Port VSWRs are to

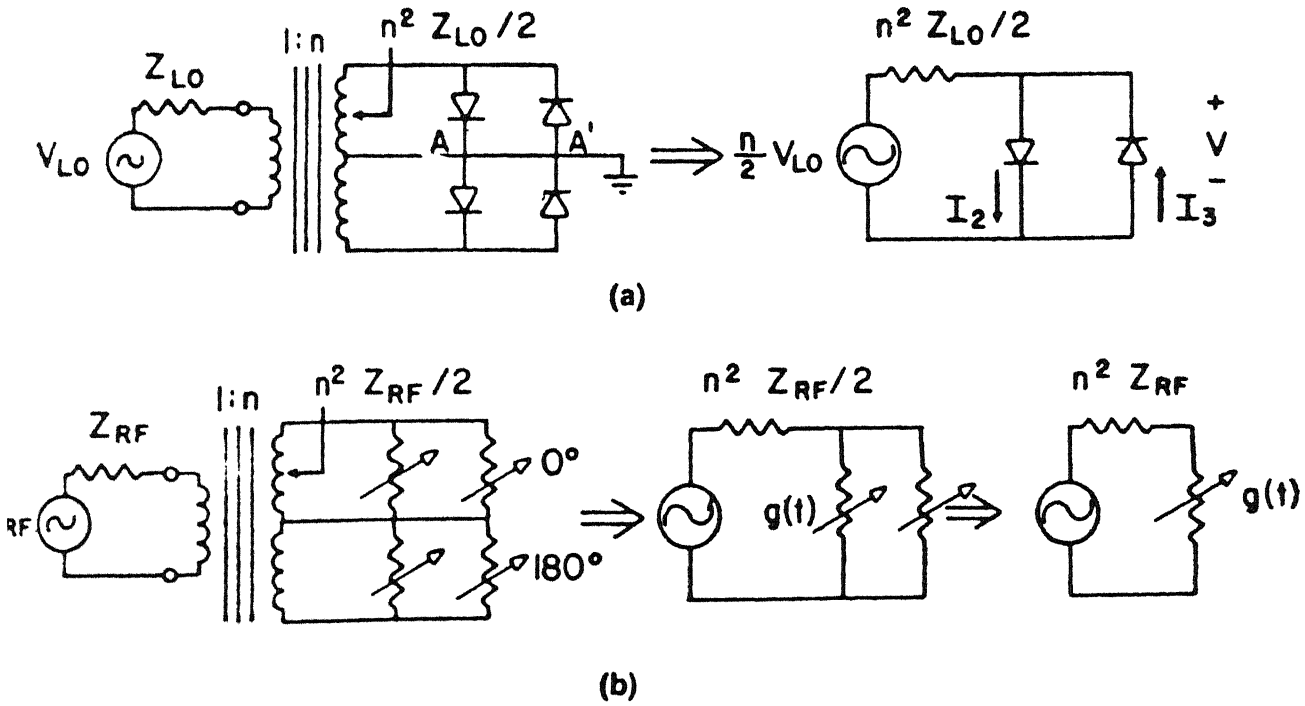

Fig 2.12(a). LO equivalent circuit for ring mixer.

Fig 2.12(b). RF equivalent circuit of ring mixer.

be reasonably good.

(f)Equivalent single diode mixers

Despite the fact that the balanced mixer design is very different from a single diode mixer, their principle of operation is same. It is possible to reduce any single balanced mixer to an equivalent single diode mixer, which has the same conversion loss and noise temperature. For a double balanced mixer design it is possible to reduce it to an equivalent two diode mixer. Then further studies can be carried out. Fig 2.12(a) shows schematically the LO equivalent circuit of a ring mixer. The virtual ground points are shown as real ground connections. It is clear from the figure that it can be divided into two separate sub circuits, each sub-circuit with two anti-parallel diodes. The currents I_2 and I_3 through the diodes can be given as

$$I_2 = aV + bV^2 + cV^3 + ...$$

$$I_3 = -aV + bV^2 - cV^3 + ...$$

where, V is the total voltage across the diode. The LO current is expressed as

$$I_{LO} = I_2 - I_3 = 2aV + 2cV^3 + ...$$

This does not include even powers of V, so I_{LO} does not include any even harmonics. This means that each diode creates a short circuit termination to other at each even LO harmonic. Fig 2.12(b) shows the RF equivalent circuit. RF equivalent circuit reduces a ring mixer into a pair of diodes and finally to a single diode with associated embedding impedances.

CHAPTER 3

DOUBLE BALANCED MIXER

3.1 DESIGN CONSIDERATIONS

Double balanced microwave mixer can be realized in MIC form using a ring quad. The DBM circuit can be configured considering various performance indices. This has been dealt in detail in chapter two. However keeping broad band operation as a main consideration ,the circuit is configured with the components having broad band characteristics.

A broad band power divider can be realized by various methods. This has been reported by Wilkinson [14] and Cohn[15]. A wilkinson's power divider offer a band width of one octave. It has got an equal phase characteristics at each of it's output port as shown in fig 3.1.

The output port isolation is obtained by series terminating the output port. Each quarter wave line has characteristic impedance of $\sqrt{2\ z_o}$ and the output is terminated by $2\ z_o$ ohms ,z_o being system impedance. This design is frequency sensitive due to it's λ_g component in the configuration. Multi section Wilkinson coupler proposed by Cohn [26] is shown in fig 3.2. A multi-section coupler consists of a large number of quarter wave sections with resistive terminations. The characteristic impedance of the sections are obtained from the normalized

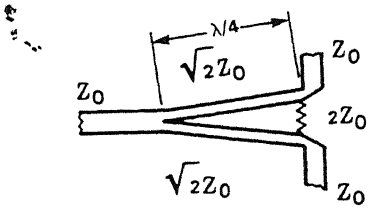

Fig 3.1. Single section Wilkinson's coupler.

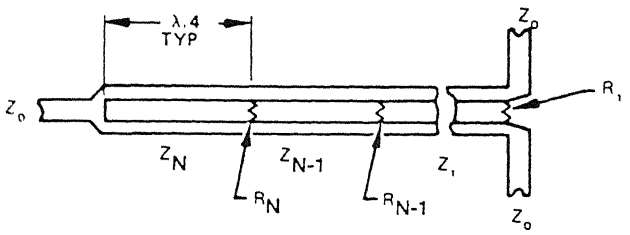

Fig 3.2. Multisection Wilkinson's coupler.

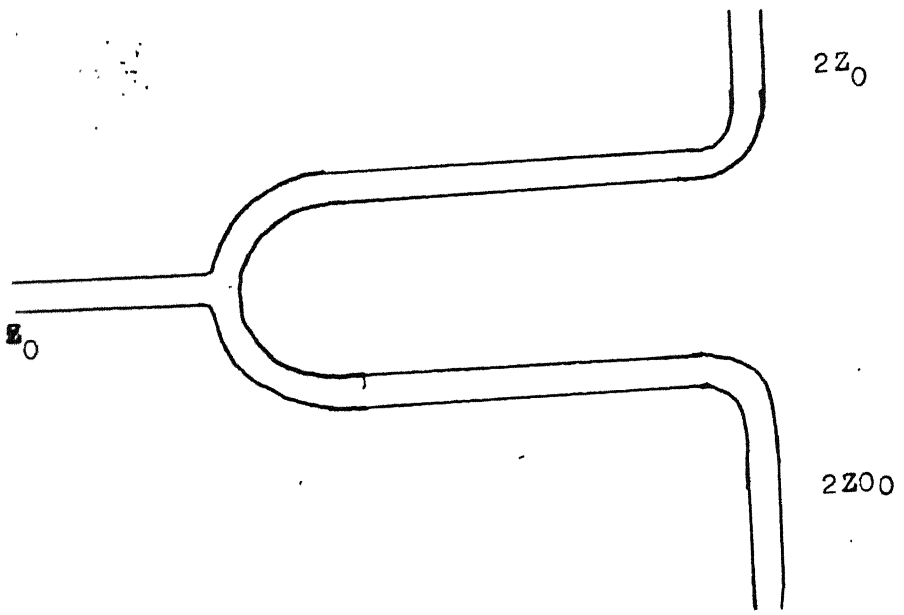

Fig 3.3. Single section frequency independent power divider.

impedances for $\lambda/4$ transformer sections for a 2:1 transformer. However all these designs have a draw back of their frequency sensitivity. The power divider used in this configuration is required to operate over a broad band. This is achieved as shown in fig 3.3. This circuit has no frequency sensitive components. Hence suitable for broad band operation.

The most important criteria in selection of the transition is to have a low return loss over a broad band. B.Schiek [8] reported transition between slot line and microstrip circuit has been found to give a band width of 1 to10 GHz. This is less frequency sensitive. Therefore, this was considered for design of the mixer circuit. Few other transitions reported by de Ronde[21] was also tried out. Various performance characteristics are provided in this chapter.

3.2 CIRCUIT CONFIGURATION

Double balanced mixer (DBM) can be realized in MIC form in several configurations. The configuration adopted for this work mainly consist of a ring quad double balanced mixer (A) as shown in fig 3.4. Ring quad is driven by the CPW (B) and CPW being excited by a slot line(C) and microstrip line (D). RF power is fed through a microstrip line (E) and then through a transition (F) to the slot line (C). LO power is fed through a microstrip line (G). The LO power is equally divided by a slot line (H) power divider. This is fed through a microstrip line (D) to the center strip of the CPW. The configuration mainly consists of

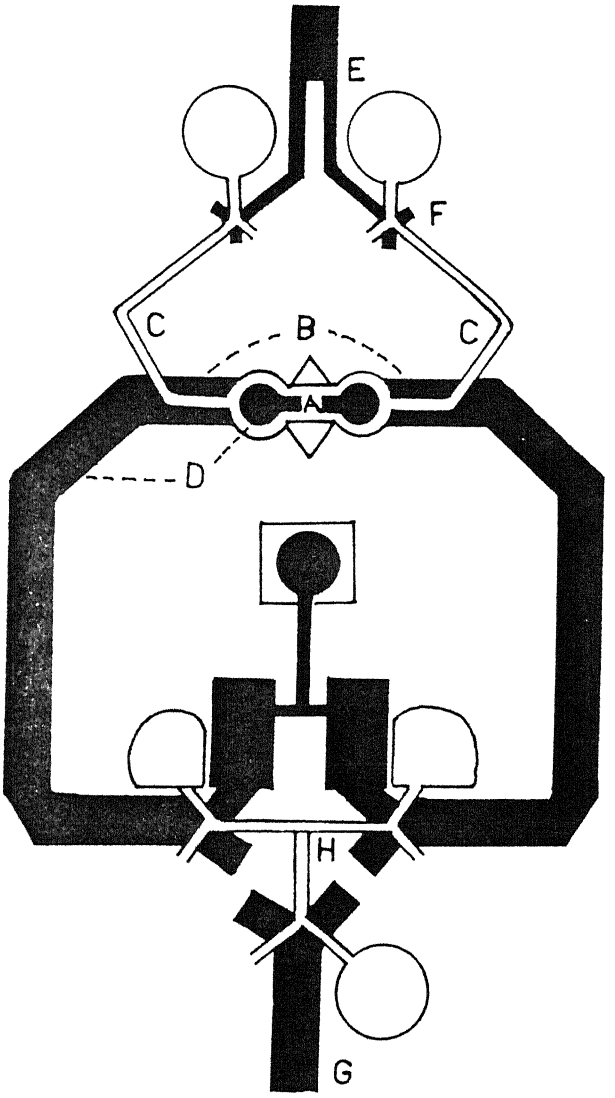

Fig 3.4. Double balanced mixer circuit configuration.

the following:

(i) Ring quad driver

The ring diode quad is driven by a CPW/CPW junction. The CPW/CPW junction is appropriate to drive a ring quad. The E field appearing across the diodes will be RF+LO and RF-LO. This is appropriate to feed a balanced input.

(ii)Uncoupled slot and microstrip junction

The slot line and the microstrip have a junction at both ends of the CPW. It is desirable that the slot line and the microstrip should be isolated as shown in the fig 3.5. As long as the microstrip and the slot line run parallel they are isolated ,as the E fields of both are orthogonal to each other. To separate these two lines , carrying LO and RF powers ,it is required to have an uncoupled junction of slot line and micro strip. It is generally not possible to have an uncoupled junction. The coupling can only be minimized. Such a junction has been designed experimentally.

(iii) Slot line microstrip transition

Five transitions have been shown in the fig 3.4. Different types of transitions have been analyzed ,fabricated and tested. The best performed transition is accepted for this thesis work.The transition selected have a broad band width.

(iv) Power dividers

Two power dividers are used in the configuration as shown in fig 3.4,the microstrip power divider as E and slot line power divider as H.The microstrip power divider is used for RF port and the slot line power divider for the LO port input. It is desired that the RF to be applied in the same phase and the LO in the

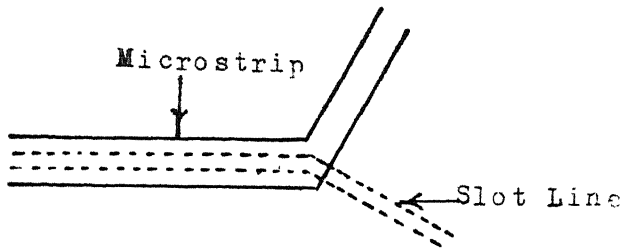

Fig 3.5. Uncoupled Slot and Microstrip junction.

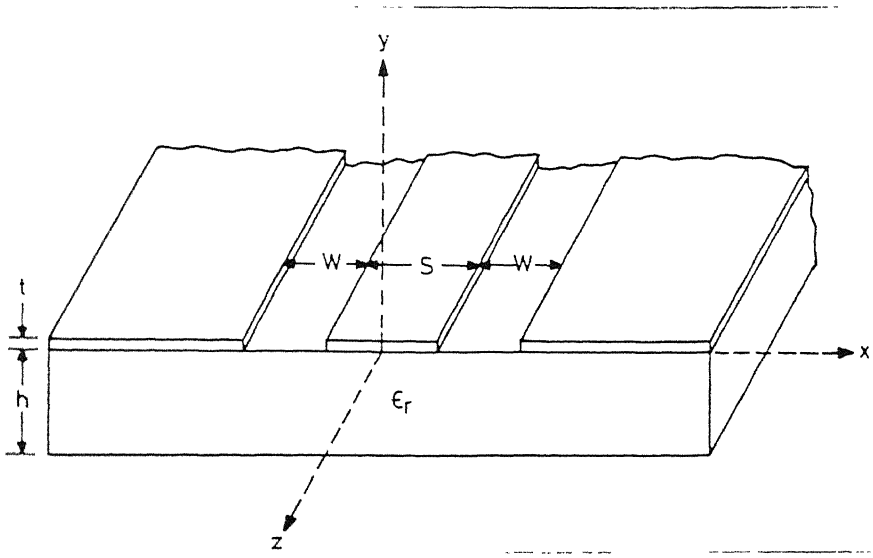

Fig 3.6. Coplanar wave guide structure.

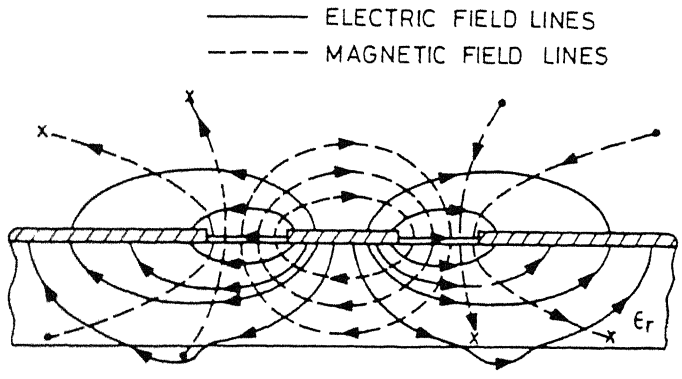

Fig 3.7. electric and magnetic field distribution in CPW.

opposite phase. There-fore, this out of phase signal for the mixer is provided by the slot line power divider in the LO path.

3.3 CPW/CPW JUNCTION AS RING QUAD DRIVER

The coplanar wave guide (CPW) is shown schematically in fig 3.6. It consists of a center strip with two ground planes located parallel to and in the plane of the strip (i.e. on the same surface of the dielectric slab). The electric and the magnetic field distribution is shown in fig 3.7. This has been dealt in detail by Gupta et al.[7]. The CPW/CPW junction is found to be useful as ring quad driver. The circuit uses an unbalanced mode LO input and a balanced mode RF input. Fig 3.8 shows the details of a CPW/CPW junction. The odd mode LO input at A and C are opposite in phase and even mode RF inputs at both A and C are in phase. When LO voltage is positive i.e. in positive half cycle of LO ,diodes D1 and D2 are forward biased and they will conduct. The diodes D3 and D4 are reverse biased ,so turned off. The diodes D1 will have RF+LO and diode D2 will face RF-LO voltages across them. The currents i_1 and i_2,in diodes D1 and D2 are different. They are given by $i_1 = i_1 + i_{RF}$ and $i_2 = i_1 - i_{RF}$ where i_1 is the LO current and i_{RF} is the RF current.

In the other half cycle i.e. negative LO cycle point A and C will change their polarity and the field across each diode will change. At that time diodes D3 and D4 will be forward biased and the field across D3 will be RF-LO. The field across D4 will be RF+LO. In exactly the similar manner the currents i_3 and i_4 in

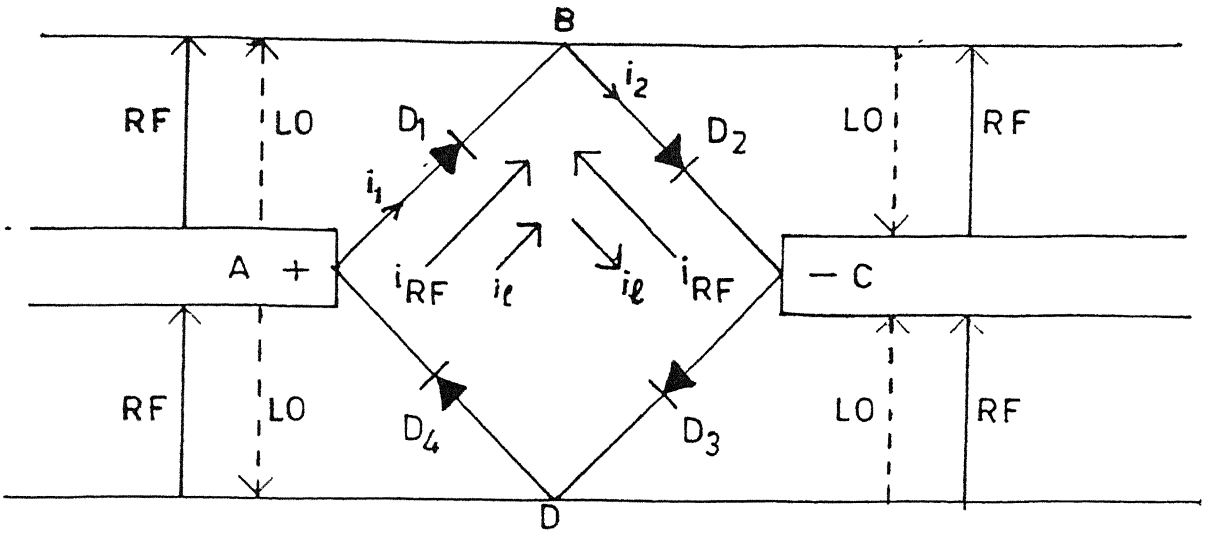

Fig 3.8. CPW/CPW junction as a ring quad driver.

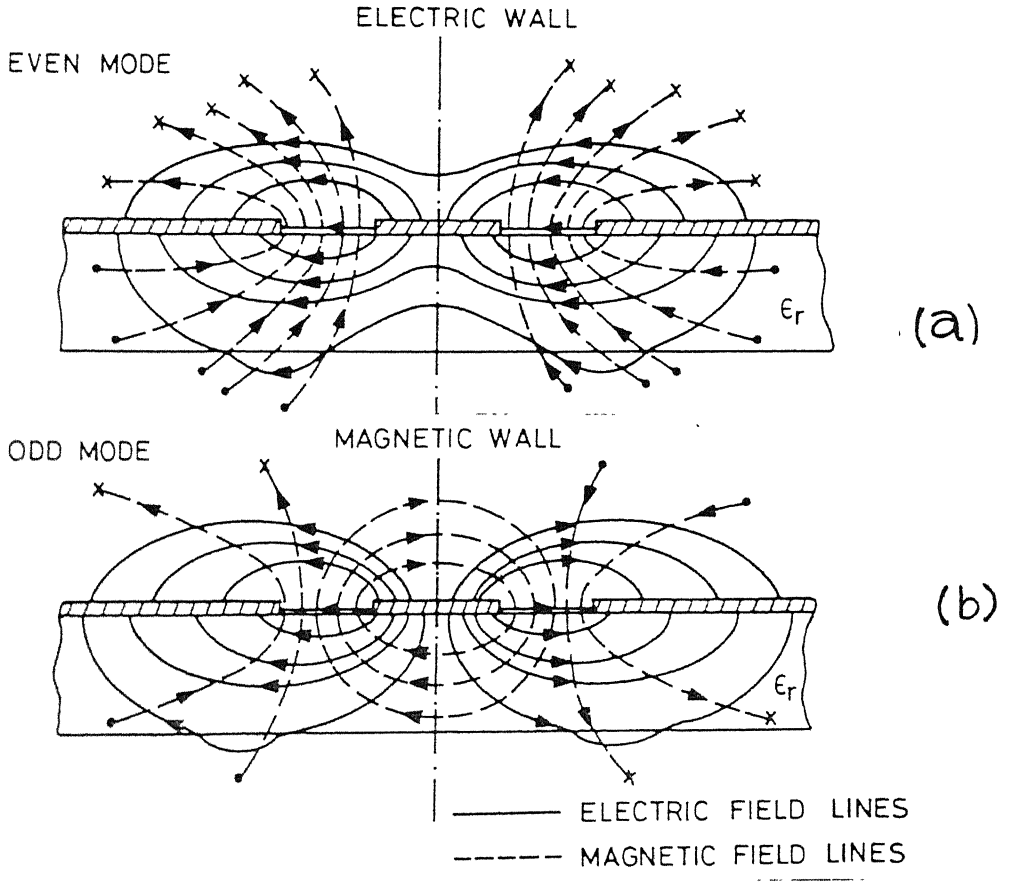

Fig 3.9. Even Mode and Odd Mode electric field configuration.

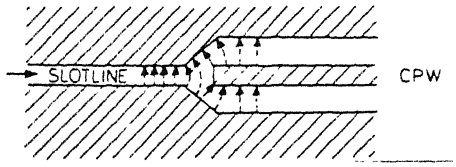

fig 3.10. Excitation of a balanced mode in CPW by Slot line.

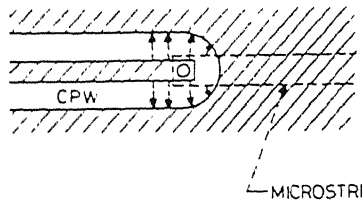

fig 3.11. Excitation of unbalanced mode in CPW by a Microstrip line.

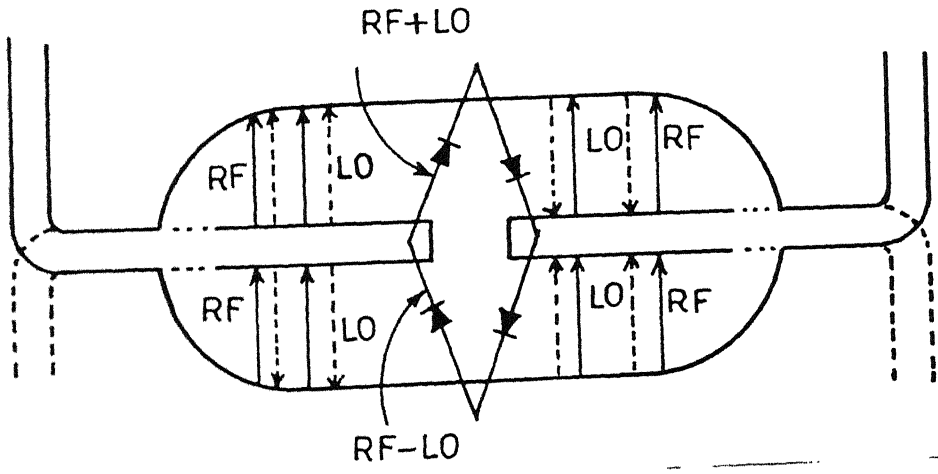

fig 3.12. A CPW arrangement for excitation of Even and Odd modes.

diodes D3 and D4 are different and are given by $i_3 = i_1 + i_{RF}$, $i_4 = i_1 - i_{RF}$.

3.4 EXCITATION OF EVEN/ODD MODES IN CPW

Fig 3.9(a)and (b) shows the electric field configuration for even and odd modes respectively. In even mode the electric field lines extend across the slot while the magnetic field lines are perpendicular to air dielectric interface in the slot.

In the odd mode the electric field lines extend across the slot as shown in the fig 3.9(b). It is seen that the plane of symmetry for the odd mode corresponds to a magnetic wall. The electric and magnetic field in the right half of the structure are in a direction opposite to the electric and magnetic field in the left half of the structure. Further, part of the magnetic field lines encircle the center conducting strip separating two slots.

A CPW when coupled to a slot line , a balance signal will propagate. This is shown in fig 3.10. If a CPW is excited by a microstrip , an unbalanced signal is launched. This is shown in fig 3.11. Therefore a combination of microstrip -CPW- slot line is used for the balanced mixer configuration. An arrangement for excitation for a double balanced mixer using CPW is shown in fig 3.12.

The RF is fed through a slot line and LO through a microstrip line to the center conductor of CPW. LO fed from both ends are

in phase opposition and RF fed from both end are in phase. So the RF propagates as a balanced mode or even mode where as the LO propagates as an unbalanced mode or odd mode ,thereby the diodes receive RF±LO accordingly.

The CPW is designed keeping in view the diode impedances. The CPW is excited by an even mode at the slot line and odd mode at the microstrip line. Therefore, the impedances seen by the CPW will be even mode impedance Z_{oe} and odd mode impedance Z_{oo}. The equivalent circuit with even and odd mode impedances are shown in fig 3.13(a) and (b). The diode impedance is required to match this microstrip and slot line odd and even mode impedances.

As already been discussed a four diode ring circuit can be converted to a single diode equivalent circuit, the single diode impedance (D as shown in fig 3.13) is required to match with the even and odd mode impedance. From the fig 3.13 it is clear that Z_{oo} and Z_{oe} are equal. But, as per [18] $Z_o = (Z_{oe}Z_{oo})^{1/2}$. Therefore, the Z_{oo} and Z_{oe} are not equal. However, keeping Z_o fixed and configuring the CPW with Z_{oe}= 65Ω and Z_{oe}=40Ω the required Z_o value is achieved.

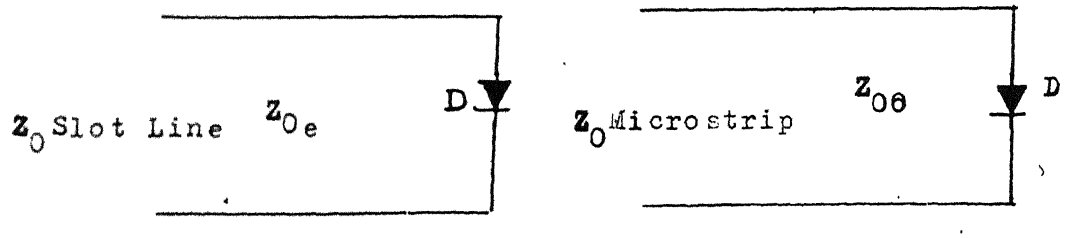

(a) (b)

...even mode and Odd mode slot line and microstrip impedance.

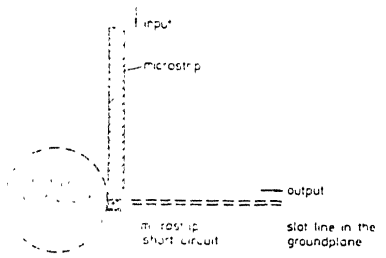

. .ig. Standard method for design of a microstrip-slot circuit.

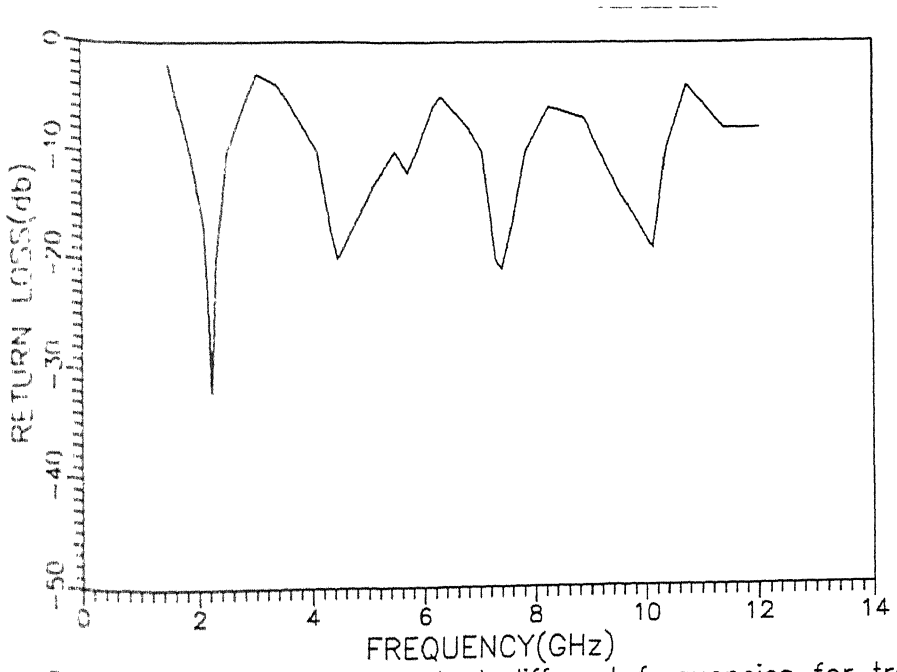

Fig 3.15 Return loss measured at different frequencies for transition No 1 .

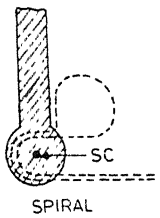

Fig 3.16. Spiral transition of Slot-Strip.

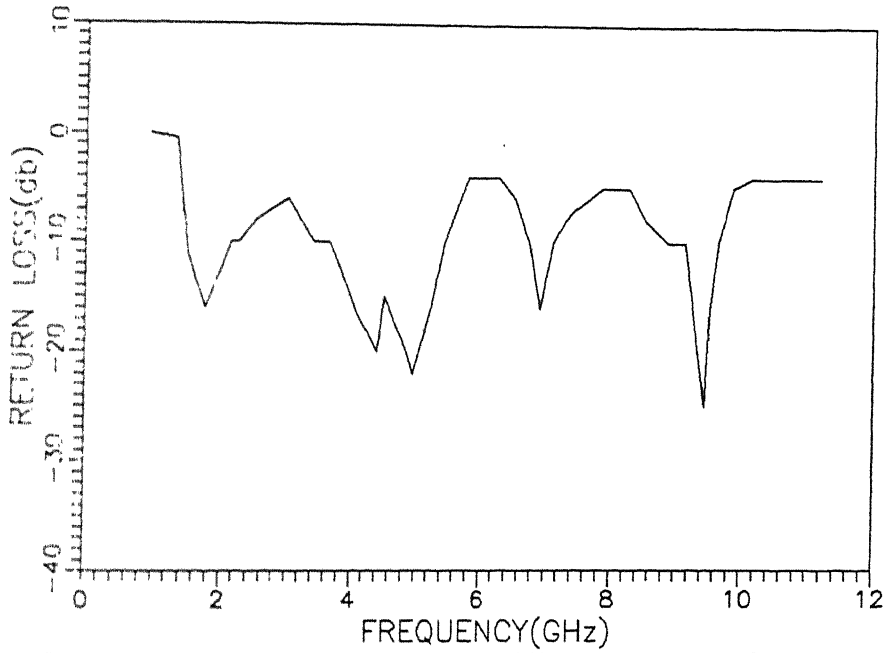

Fig 3.17 Return loss measured at different frequencies for transition No 2 .

3.5 SLOT LINE TO MICROSTRIP TRANSITION

Microstrip transmission line in combination with slot lines have been used in this project work. A very important factor in the strip-slot circuitry is well matched strip-slot transition with low insertion loss. This transition can be achieved by several methods. Fig 3.14 shows one of the designs. In this design the slot line open circuit is realized by a circle and the short circuit of microstrip is realized by physically shorting the microstrip with the ground plane. The return loss characteristics of the transition is shown in Fig3.15. This transition showed insertion loss very high and low bandwidth. The reason for non optimum behavior of this transition may be due to mechanical restrictions and improper alignment.

The other type of transition which was fabricated and tested is shown in fig 3.16. Here the strip end was circular and was shorted to the ground plane physically. The slot line which had a spiral coil was placed below microstrip as shown in figure. Slot line open circuit was realized by a circle. The return loss characteristics is shown in fig 3.17. This transition again was band limited due to mechanical restrictions.

It has been reported [8] that a slight modification of the strip slot transition of fig 3.16 makes the position of microstrip short circuit plane and the slot open circuit plane far less critical and improves the overall performance of the transition.

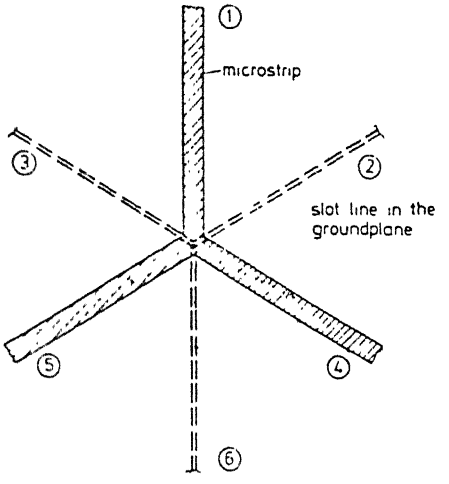

...4. 4-port junction used in an improved micrstrip-slot line transition.

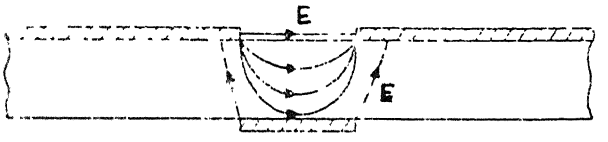

------ FIELD CONFIGURATION IN MICROSTRIP

——— FIELD CONFIGURATION IN SLOTLINE

...4.14. Coupling of electric field from microstrip to slot line.

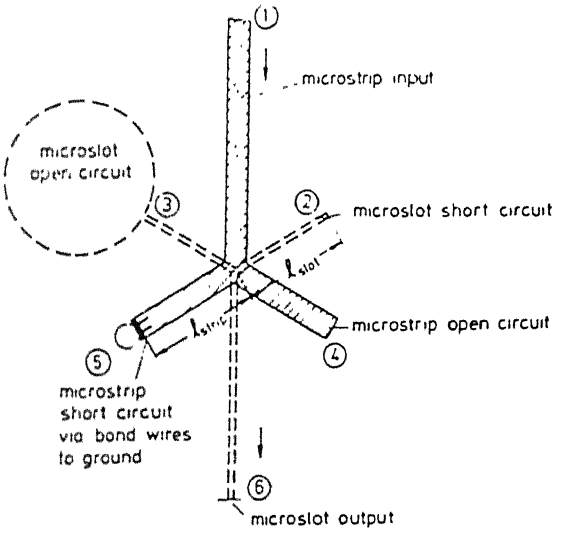

...15. Microstrip-slot line transition with open and short circuited lines.

In order to explain the necessary modifications, one may start from the double junction of fig 3.14. A six port junction used in an improved microstrip slot line transition is shown in fig 3.18. This circuit is matched at port 1 and port 6 when

- the ports 2 through 5 are terminated by matched loads
- the characteristic impedances of all the microstrips and slot lines are equal.
- the junction effects can be ignored.

It is seen that there is no direct coupling between port 1 and port 6. This could be explained qualitatively on the basis of field configurations for microstrip (at port 1) and the slot line (at port 6) shown in fig 3.19.

The two lines are collinear. It is seen that the 'E' field of microstrip has even symmetry while that of slot line has odd symmetry. thus there is no net coupling. Examining the equivalent circuits as seen from port 1 and port 6, looking from port 1, the slot lines leading to port 2 and port 3 are parallel to each other and in series to the two parallel microstrip lines that lead to port 4 and port 5. Thus input impedance from port 1 is 50Ω. Similarly, looking from port 6, the slot lines leading to port 2 and port 3 are in series to each other and parallel to the series connected microstrip lines that lead to port 4 and port 5. Thus, also looking from port 6 the input impedance of junction is 50Ω. In a similar manner it can be proved that the input impedance of the junction is 50Ω when looked from any port. Also, under these conditions port 1 and port 6 are decoupled. If a signal is incident at port 1, the signal will be equally

distributed into ports 2 to 5. If ports 2 to 5 have same reflection coefficient, then the signal will be reflected back into port 1. Similarly an input signal at the slot side (port 6) will also be equally transmitted into ports 2 to 5, but in phase opposition at port 2 and port 5 with respect to port 3 and port 4.Again an equal reflection coefficient at port 2 and port 5 will reflect signal back into port 6. Therefore, a reflection coefficient of $\exp(j\phi)$ at port 2 and port 5 and of $\exp(j\phi+180^{\circ})$ at port 3 and port 4 causes a perfect transition of input signal (port 1) into the output port 6. Fig 3.20 shows realization of this transition with short and open circuits.

The length l_{slot}, and l_{strip} are the distance from the short or open circuit to the center of the structure. For the above condition to hold, the electrical lengths of the lines from the open or short circuits to the center should be equal to $\beta_m l_m = \beta_s l_s = \theta$, where, β_m and β_s are phase constants and l_m and l_s are line lengths for microstrip and slot lines respectively. In the experimental realization l was made very small. The distances from short circuit to open circuit i.e, 21 should be less than $\lambda/4$ in order to reduce radiation effects.

If the impedances of the microstrip and slot lines are different then the transition impedance can be expressed as $Z_{om}\tan\beta_m l_m$ and $Z_{os}\tan\beta_s l_s$, where, Z_{om} and Z_{os} are characteristics impedances of microstrip and slot lines respectively. The return loss characteristics of this type of junction is shown in fig 3.21. It gives a wide band

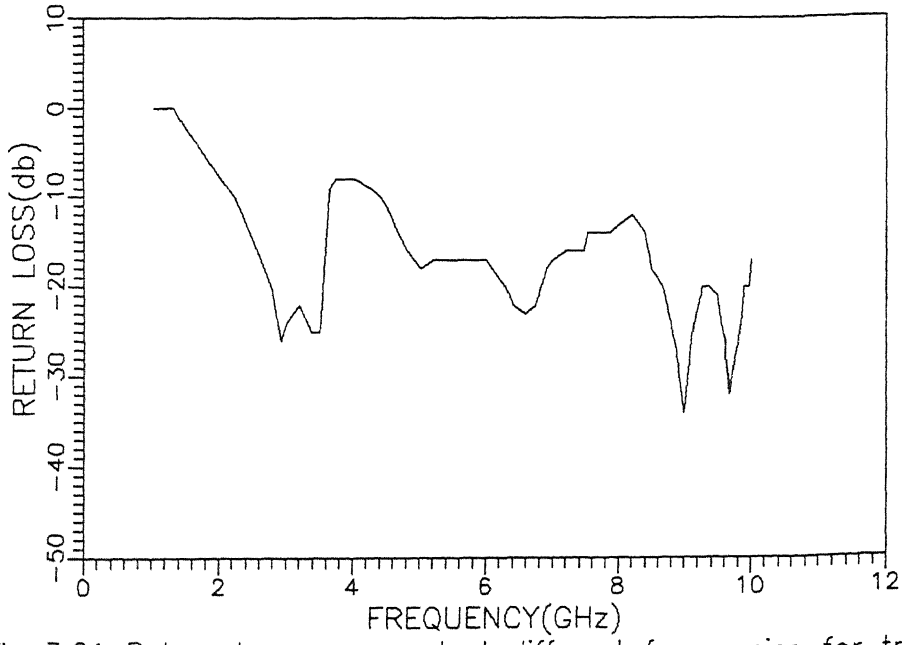

Fig 3.21 Return loss measured at different frequencies for transition No 3

characteristics. Hence, this was selected for this work.

3.6 SLOT LINE MICROSTRIP JUNCTION WITH MINIMUM COUPLING

The RF signal is fed through the slot line and the LO signal is fed through a microstrip line for exciting even and odd modes in the CPW, the slot line and microstrip lines have to be collinear at the excitation end. As long as the slot line and microstrip lines are collinear, there is no coupling of fields as the electric fields are orthogonal. As they depart from each other, part of the electric field couples from one transmission line to the other, which is undesirable. For the present work two types of junctions which gives minimum cross coupling between the lines are studied. The first type is shown in fig 3.22(a). Here, the microstrip and slot lines diverge at right angles. In the other configuration the microstrip and the slot lines are taken with an angle of 120° to each other as shown in fig 3.22(b). Two circuits with 90° bend and 120° bend were designed. the printed circuit board layout in shown in fig3.23. The microstrip was feeding the slot line. The previously discussed slot/microstrip transitions have been used for feeding the slot line via coaxial input. The compensation has been provided at the bends as per design criteria given in [6]. S - parameters have been measured for these two configurations. These characteristics are as shown in figures 3.24(a) and 3.24(b).

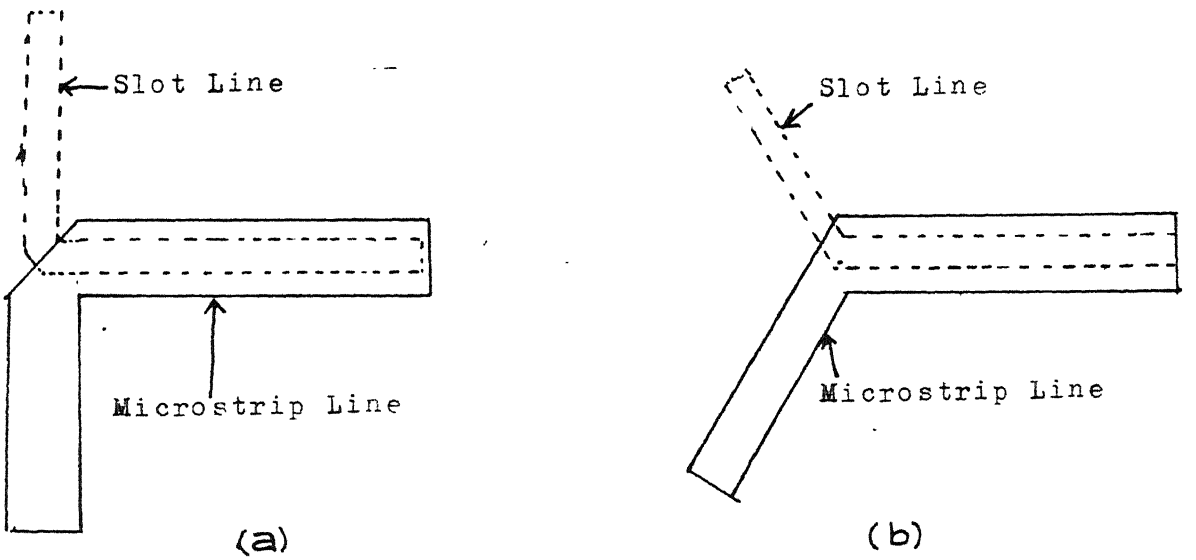

Fig 3.22. Microstrip and Slot line uncoupled junction.

(a)Bend of 90 degree.

(b)Bend of 120 degree.

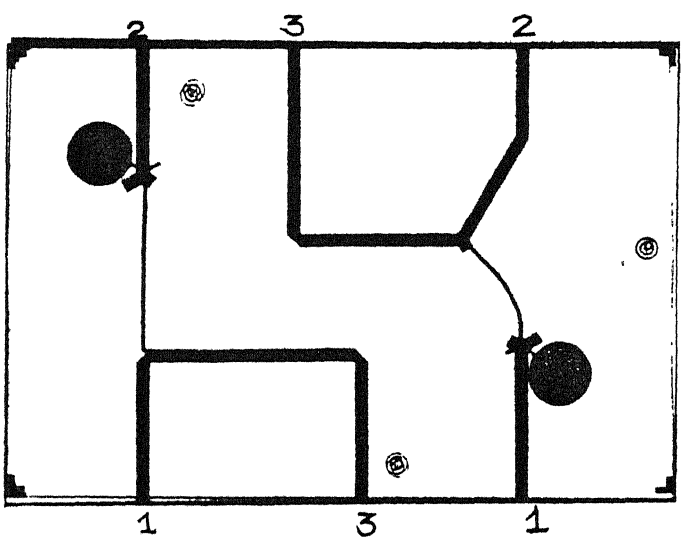

Fig 3.23. Printing pattern for 90 degree and 120 degree Microstrip Slot line Uncoupled junction.

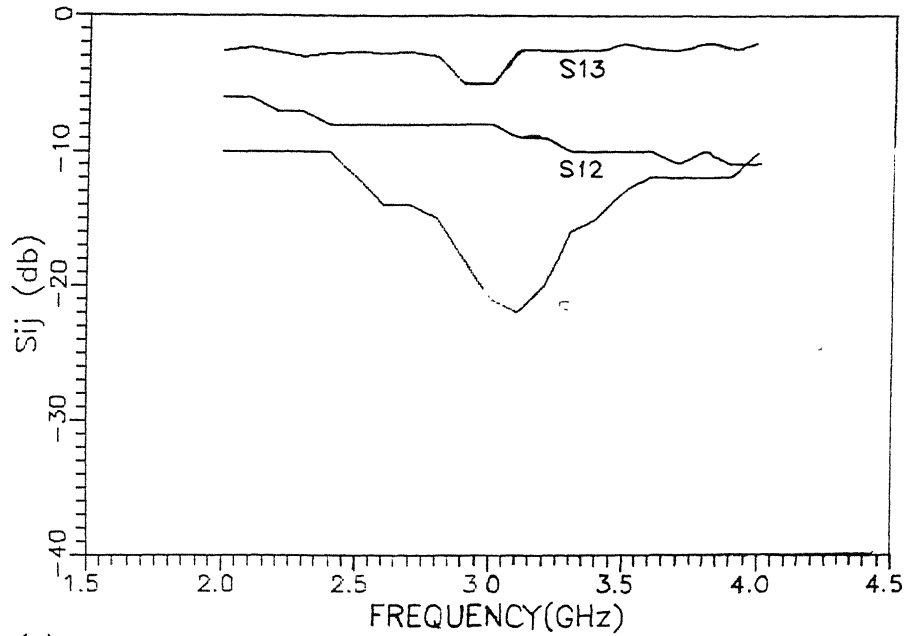

Fig3.24(a)Measured S-parameters for different frequencies for 90 degree bend

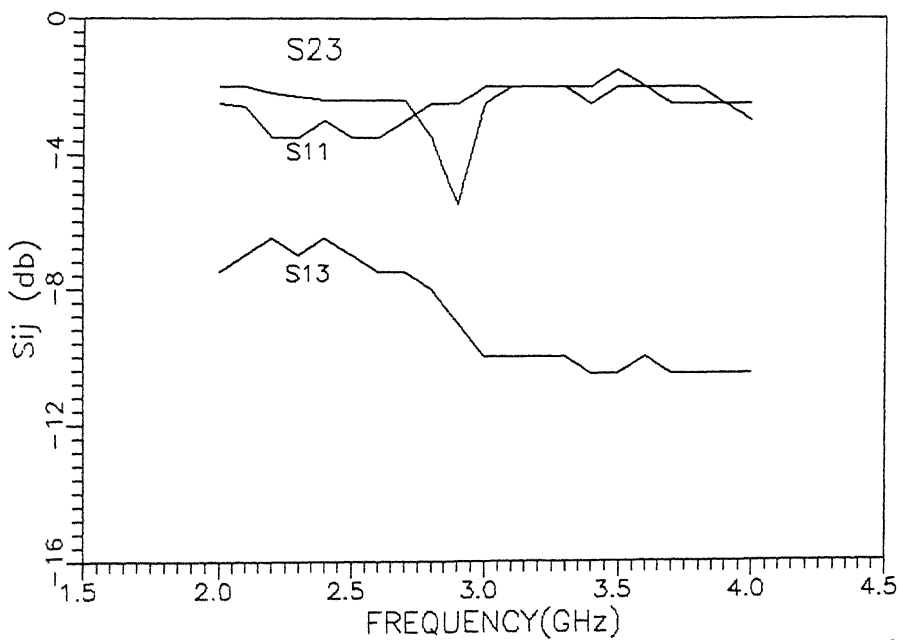

Fig3.24(b)Measured S-parameters for different frequencies for 120 degree bend

CHAPTER 4

DESIGN AND PERFORMANCE CHARACTERISTICS OF THE DOUBLE BALANCED MIXER

4.1 INTRODUCTION

The printing of the circuit was under taken at the PCB laboratory with existing facilities. The fixture fabrication was under taken at the departmental Workshop. The testing of the mixer circuit was carried out in the departmental laboratory with existing test equipment. The printed circuit pattern is shown in fig 4.1. The design details of the transitions , power dividers , and other components are dealt in this chapter. The various performance characteristics are also included in this chapter.

4.2 DESIGN OF DOUBLE BALANCED MIXER

The configuration adopted has already been discussed in chapter 3. In the present configuration the design of the CPW is most critical. The diode impedance is to match to the even and odd-mode impedances of the CPW. All other transmission line impedances are to match with this impedance. As discussed in chapter 3 the odd-mode impedance (Z_{oo}) was assumed 40 ohms and even mode impedance (Z_{oe}) was assumed to be 65 ohms to match the diode impedance. Keeping this in mind the existing transmission

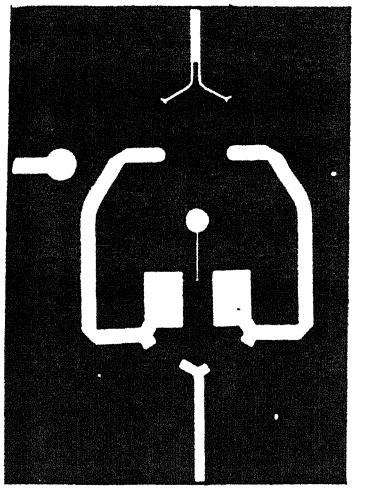

(a)

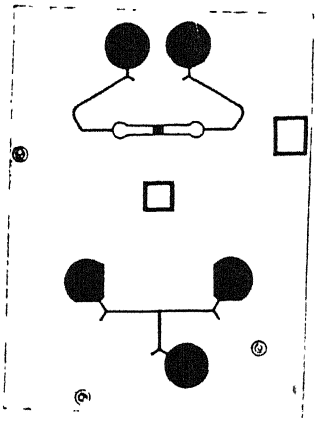

(b)

Fig 4.1. Printed circuit pattern .

(a) Microstrip side .

(b) slot line side.

line impedances ,slot line for even mode and microstrip for odd-mode are designed. The 40 ohm microstrip is used to excite odd-mode in CPW and a 65 ohm slot line exciting even-mode of CPW. The slot line characteristics impedance is a function of frequency and we cannot maintain a fixed 65 ohm impedance over the entire band width of interest. Therefore, the slot line is designed to be 65 ohm at the mean frequency, approximately 5 GHz. The LO and RF inputs are required to be of 50 ohm impedance and the RF power is divided into two paths with equal phase and LO is divided into two paths and in phase opposition. This is achieved by having a microstrip power divider for RF and a slot line power divider for LO , which has out of phase power division property. However, due to evanescent modes and reflections from the 90 degree bends the voltage division in slot line power divider in the output ports are not exactly half of the input port. The evanescent mode contribution at the junction can be modeled as an equivalent inductance /capacitance network , which gives rise to an impedance transformation in addition to power division. This case is comparable to that of a 90 degree 'T' bend of a waveguide where the output voltage is not exactly half the input voltage. The 90 degree slot line power divider case is some what similar. The design details of the slot line power divider was not readily available. Therefore, we have resorted to some empirical approximations and arrived at the impedances of the slot line as 62 ohms input and 55 ohms output lines These values gave practical dimensions to the slot lines, further, the performance aspects of slot line power divider were not evaluated accurately because , we can tolerate some VSWR at the LO port. A

transition with impedance transformation from 50 ohms microstrip to 62 ohm slot line is designed so that input port for LO can be connected to a microstrip to coaxial transition. The 55 ohms output ports of the slot line power divider are matched to 40 ohms microstrip line through a broad band transition and impedance transformer.

The 65 ohms slot line of CPW junction is connected by 65 ohms slot line at both ends to feed the RF in even mode. The RF signal is fed through a 50 ohms microstrip to coaxial transition. The requirement for a CPW/CPW is an in phase signal at both ends for the RF signal. Therefore, a microstrip power divider, to feed in phase signal is designed. The 65 ohms slot line and the output ports of the microstrip power divider are matched through a transition and impedance transformation. The design of the entire circuit can be broadly divided into following parts.

(a) Design of CPW junction for driving the quad

(b) Design of slot line /microstrip transitions with impedance transformations and various transmission lines

(c) design of power dividers

(a) design of CPW junction for driving the quad

The CPW is designed keeping in view ,the diode impedances. The diode impedance with a drive level of 5 mW is measured approximately to 50 ohms. The odd-mode and even-mode impedances have been assumed to be 40ohms,65 ohms respectively in chapter 3. The even-mode is excited by the slot line and the odd-mode is excited by the microstrip line. Therefore, for

matching, the input microstrip should have 40 ohms and slot line should have 65 ohms as the characteristic impedances.

For the even-mode , the metal strip between the slots has little effect on propagating waves. The wave propagates as if it were in a slot of width (2 * slot width + microstrip width) [7]. Keeping a slot width of.2 mm and micro strip width of 1mm,the value of 2* slot width + microstrip width becomes 1.4 mm. Referring, [6] for slot line with s/h value as 1.4/1.3 the characteristic impedance is found to be 130 ohms. Thus even-mode impedance is half of this value which becomes 65 ohms.Therefore, the assumed value of slot width for even-mode impedance is found correct.

For the odd-mode impedance referring, [6] for CPW transmission line static characteristics for 40 ohms of impedance and h/d of 0.92 , the w/d value is found to be 0.71. Therefore, the width of the microstrip is.994mm.

(b) Design of transitions with impedance transformation and transmission lines.

(1) Design of transition with impedance transformation

(i) design of 100 ohm micro strip to 65 ohm slot line transition with impedance transformation.

The phase constant for 100 ohm microstrip is β_{100m}

The value of β_{100m} = .26 rad/mm

The phase constant for 65 ohms slot line is β_{65s}

The value of β_{65s} = 0.19 rad/ mm

Therefore, the transition with impedance transformation equation can be written as:

$100 \tan(2\pi x.26x\ l_{micro}) = 65 \tan(2\pi x.19 x\ l_{slot})$

Where l_{micro} is the length of the microstrip from it's shorting end to the junction point.

l_{slot}, is the length of the slot line from the open end to the junction point.

If l_{slot} is assumed as 1mm.

then $l_{micro} = 0.42$mm.

(ii) Design of 40 ohms microstrip to 55 ohms slot line transition with impedance transformation.

The phase constant β for 40 Ω microstrip is calculated as

$\beta_{40m} = 0.2784$ rad/ mm

The phase constant β for 55 Ω slot is calculated as

$\beta_{55s} = 0.222$ rad/mm.

For transition

$55\tan(2\pi x0.222xl_{slot}) = 40\tan(2\pi x0.2784xl_{micro})$

assuming l_{slot} as 1.5mm, l_{micro} is calculated to be 1.59mm.

(iii) Design of transition of 62Ω slot line and 50Ω microstrip line with impedance transformation.

The β for the slot line with 62Ω is

$\beta_{62s}=0.22$ rad/mm

The β for microstrip line with 50Ω is

$\beta_{50m}=0.305$ rad/mm

Therefore, this transition equation is

$50\tan(2\pi x0.305xl_{micro}) = 62\tan(2\pi x0.22xl_{slot})$

assuming l_{slot} as 1.2mm, l_{micro} is calculated to be 2.02mm.

(2) Design of different transmission lines:

(i) Design of microstrip 50Ω line.

Referring [9] the design data calculated are as follows:

H' = 2.16859172

w/h = 0.939266824

therefore, the width of the microstrip is 1.22mm

ε_{reff} = 6.76

λ_g = 23.07566 mm

(ii) Design of 100Ω microstrip transmission lines

Referring [9] the design data calculated are as follows:

H' = 4.1392483

w/h = 0.1275

therefore, the width of the microstrip is 0.16mm.

ε_{reff} = 6.1680254

λ_g = 24.1589 mm

(iii) Design of slot line with characteristic impedance 65Ω

Referring [7] the slot line data calculated are as follows

w/h = 0.23, assuming width of the slot (w) as 0.3mm

h/λ_o = 0.02166

therefore, λ_g/λ_o = 0.55093

ε_{reff} = 3.2946

λ_g = 33.0558 mm

(iv) Design of 40Ω microstrip line

Referring [9] the design data calculated are as follows:

H' = 1.7728

w/h = 1.442

therefore, the width of the microstrip is 1.87 mm

ε_{reff} = 7.0715

λ_g = 22.5629 mm

(v) Design of 55Ω slot line

Referring [7] the slot line data is calculated as follows:

w/h = 0.1538, assuming the width of the slot as 0.2 mm.

h/λ_o = 0.021666

λ_s/λ_o = 0.4711564

ε_{reff} = 4.50474

λ_g = 28.269 mm.

(C) Design of Power dividers :

(i) Design of microstrip power dividers :

RF signal is fed to the CPW in even mode in phase with the help of this power divider. Power dividers using λ/4 transformers are frequency sensitive. To achieve a broad band characteristics the frequency sensitive elements are eliminated in this design. The input port having an impedance of 50Ω divides the power in equal phase to two output ports. If the field configuration is observed the output ports will be found in parallel to the input port. Therefore, the output port impedances are fixed to 100Ω each. The length of the output ports are kept independent of the frequency.

(ii) Design of Slot line power divider :

The CPW is required to be excited by an odd mode through an out of phase LO signal. This is achieved in this configuration by the help of a slot line power divider. The slot line power divider is configured with output ports at right angles to the input port. If the E field configuration is observed the two output ports will be found in series. This case is similar to a

'T' junction in each case of a wave guide. Even though the output ports are in series, the voltage division is not exactly half at the output ports. This is mainly due to the evanescent mode and reflection from the 90 degree bend. The evanescent mode combination at the junction can be modelled to an equivalent inductance capacitance network, which gives rise to an impedance transformation in addition to the power division. This can be compared to a 90 degree 'T' bend of a wave guide where provisions of iris and stubs are available for matching the impedances. As already mentioned the power divider is designed with input port having an impedance of 62Ω and output port having 55Ω impedance.

4.3 HP 5082-2276 RING QUAD SPECIFICATION :

The 5082-2276 matched diode quads consist of a monolithic array of hot carrier diodes inter connected in ring configuration for 's' band. The four hot carrier diode junctions are isolated by a dielectric with good microwave properties and inter connected with microstrip lines of less than 20 mils length each, resulting in an interconnecting inductance of less than 0.5 nH each. Close proximity of the active junctions and a common dielectric substrate provide for inherent diode match and temperature tracking characteristics for superior to four individual diodes.

Absolute maximum rating :

Operating temperature range $-65^{o}C$ to $+125^{o}C$

Storage temperature range $-65^{o}C$ to $+125^{o}C$

DC power dissipation 75 mW

Electrical Specifications :

Capacitance G		0.6 pF
Junction Capacitance	Δ_{cj}	0.1 pF
Series Resistance	R_s	10 Ω
Breakdown Voltage	V_{BR}	2 V
SSB Noise figure	NF	6(typical)

4.4 PERFORMANCE CHARACTERISTIC OF DBM :

4.4.1 Reflection coefficient characteristics:

The reflection coefficient at RF and LO ports are measured separately. The experimental setup for the same is shown in fig 4.2.(a)

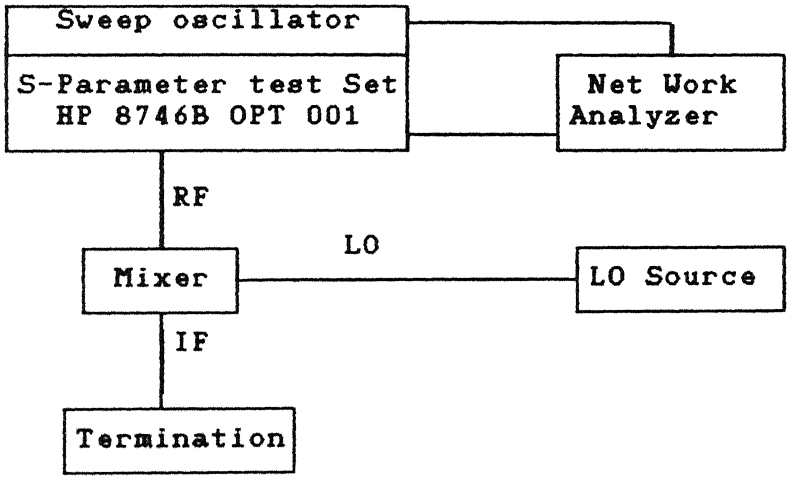

Fig. 4.2 (a) Measurement of reflection cofficient in RF port.

In the measurement of RF port reflection coefficient the network analyzer and S-parameter test set was used in conjunction with a sweep oscillator. The output of the sweep oscillator was

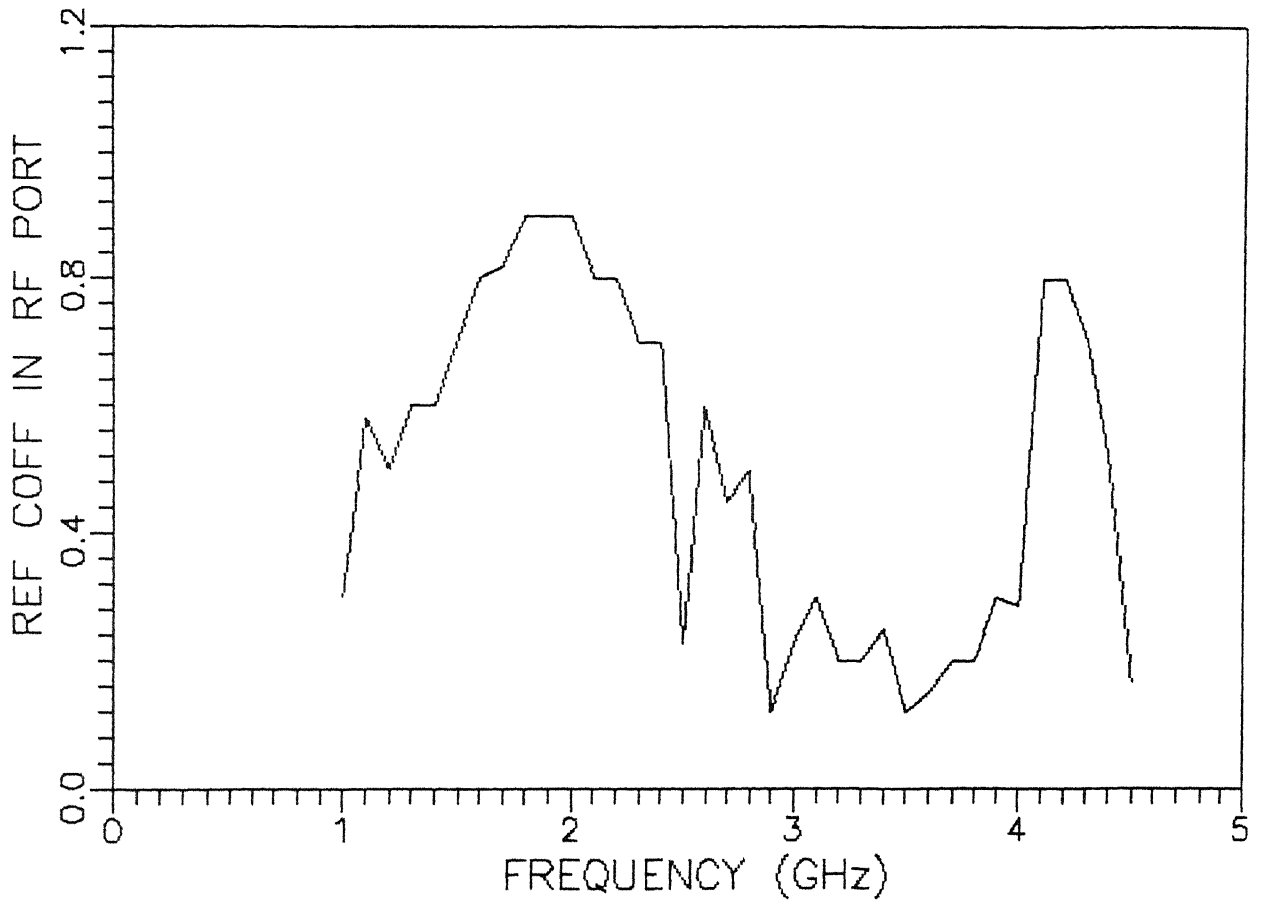

Fig4.2(b) reflection cofficient at RF port at different frequency

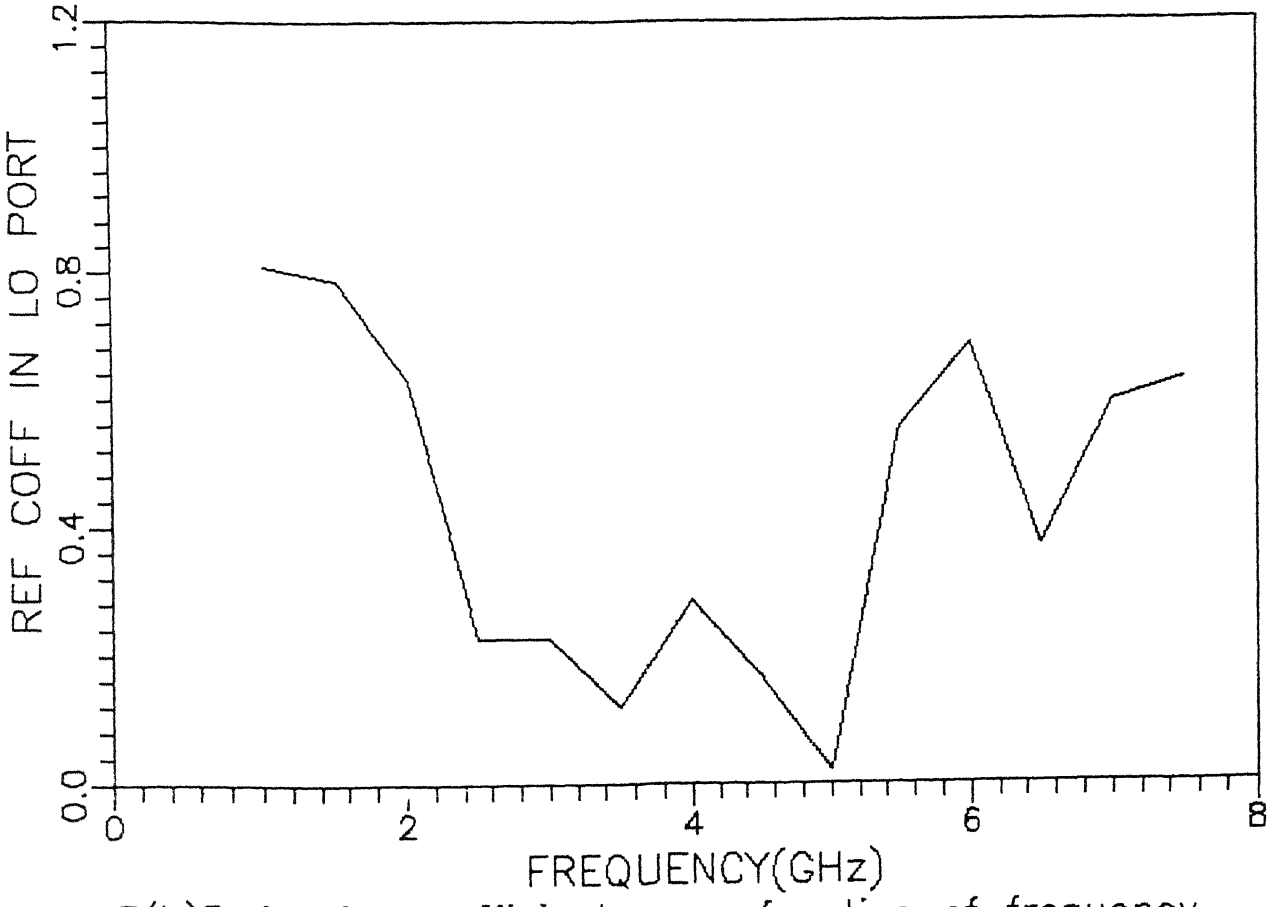

Fig4.3(b)Reflection cofficient as a function of frequency

levelled. The IF port of the mixer was connected to the oscilloscope. The RF port was connected the the S_{11} port of S-parameter test set. The results were measured on the network analyser.

The measured results are plotted in fig 4.2(b). It was observed that below 2GHz the reflection coefficient was high. The reflection coefficient was found to be within 0.25 from 2 GHz to 5.5 GHz. After 5.5 GHz the reflection coefficient was again high. The high value of reflection coefficient is mainly due to the mismatch in the circuit elements.

The reflection coefficient at the LO port was measured in the experimental setup as shown in fig 4.3(a). The mixer and RF ports are terminated with matched load when the LO port was fed from the RF source through a four port directional coupler. The incident power and reflected powers were measured at the incident and reflected port of the directional coupler. The ratio of these two powers gives the reflection coefficient. These are recorded and presented in the graph 4.3(b). The reflection coefficient was high till 2.5 GHz and it was within 0.2 from 2.5 GHz to 5 GHz. However, at higher frequencies the LO port reflection coefficient was found to be from 0.2 to 0.6.

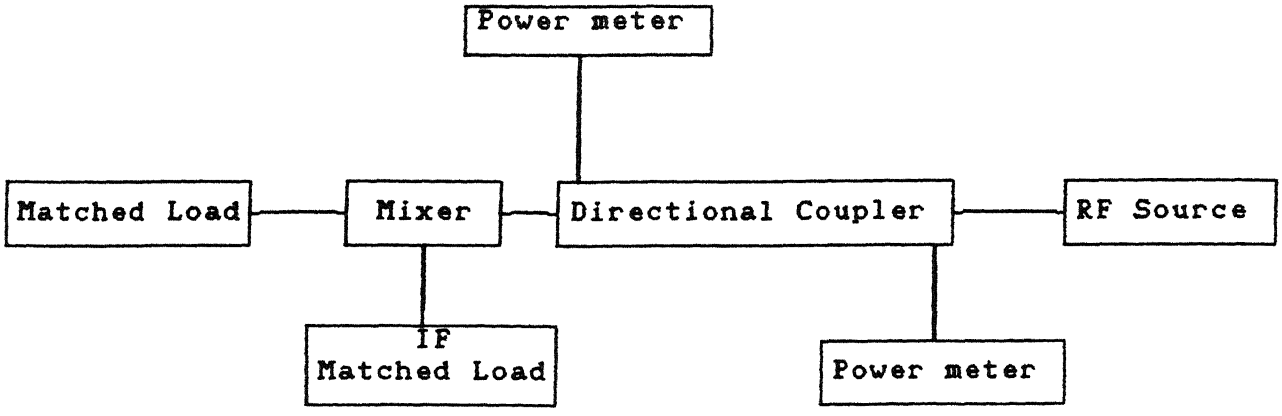

Fig. 4.3(a) Measurement set-up of input reflection coefficient at LO port.

4.4.2 Conversion loss characteristics

The measurement setup is shown in fig. 4.4(a). The signal source used for RF and LO are driven at a constant power level. The power level for LO was 10 mW. The RF signal levelled output was fed to the mixer RF port. The IF output power was measured in the oscilloscope. The IF output was measured for different RF and LO frequencies, keeping the IF frequencies at 25 MHz. The characteristics is shown in fig 4.4(b). The conversion loss was high below 2.5 GHz. From 2.5 GHz to a frequency of 4 GHz the conversion loss was found within 5.5 dB. From 4 GHz onwards the conversion loss is found increasing slowly till 5 GHz. This high conversion loss is mainly due to the quad parasitic elements. Quad is optimised for operation up to 3 GHz and above this frequency the conversion loss goes high.

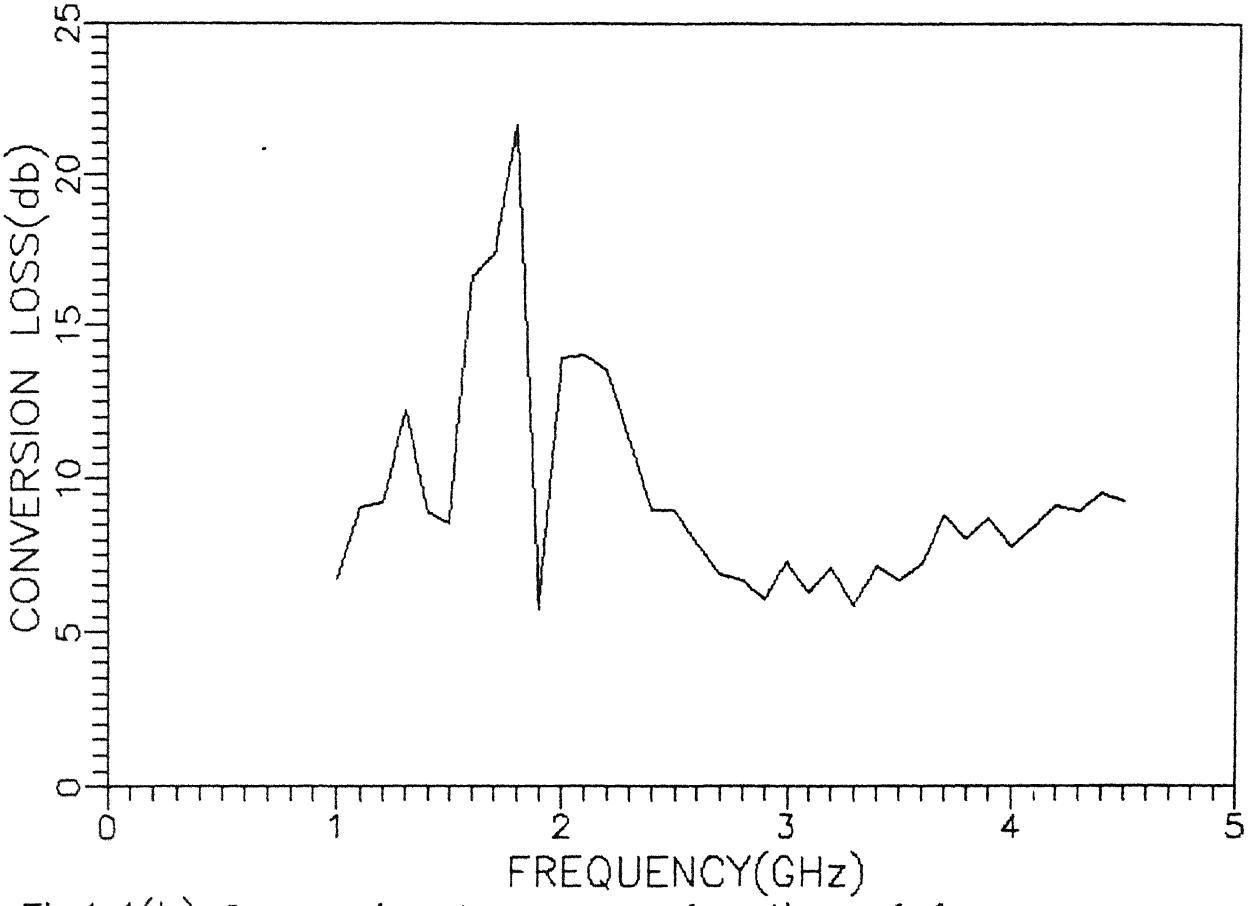

Fig4.4(b) Conversion loss as a function of frequency

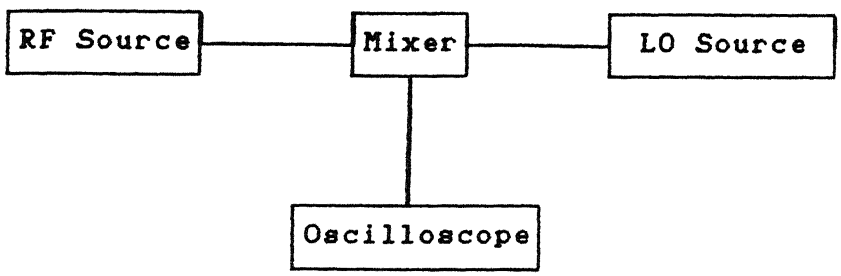

Fig 4.4(a) Experimental set-up for measurement of Conversion Loss

4.4.3 Noise Figure Characteristics :

The Noise Figure of the mixer was measured at different frequencies. The experimental set-up is shown in fig 4.5(a). The LO power is fed at a level of 10 mW. The noise figure measuring equipment used was HP 8970B NOISE FIGURE METER with a broad band noise source. RF input is fed from the noise source of the noise figure meter. The IF output was fed to the noise figure meter. At the IF frequency of 25 MHz the noise figure at different LO frequencies are recorded. The same has been presented in the graph 4.5(b). Initially, below 2.5 GHz frequency the noise figure was high. After 2.5 GHz up to 4.5 GHz the noise figure was within 8 dB. After 4.5 GHz the noise figure was observed increasing slowly.The main reason for this high noise figure is due to the higher noise figure of the diode quad above 3 GHz and also due to mismatch in the circuit.

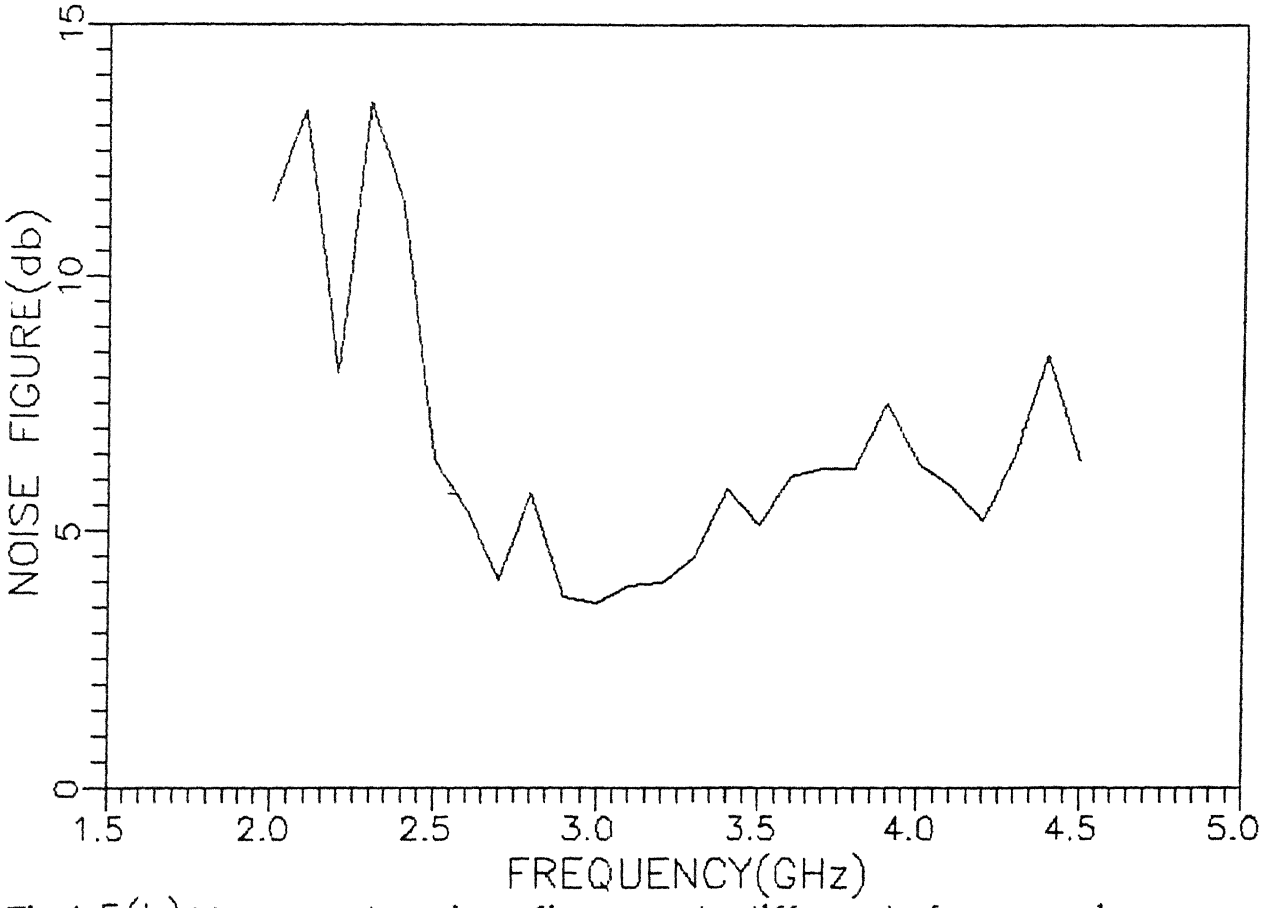

Fig4.5(b) Measured noise figure at different frequencies

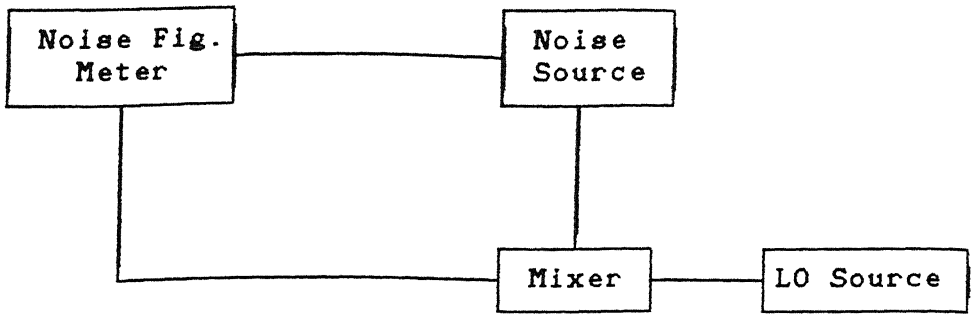

Fig 4.5(a) Experimental set-up for measurement of Noise Figure.

4.4.4 Local Oscillator Power Vs Conversion Loss :

The effect of LO power on conversion loss was measured in this set up. The experimental set up is shown in fig4.6(a). The RF signal is fed at a constant frequency at a measured level. The LO frequency is adjusted to give an IF of 25 MHz. The LO power level is varied from a minimum to a maximum. Various LO powers were measured simultaneously by a power meter through a directional coupler. The measurements are carried out at three different frequencies. The performance characteristics is presented in fig 4.6(b). It was observed that below 10 mW of LO power the conversion loss was high. It levels down on a drive level of 10 mW onwards and remains constant after about 25 mW. The change in LO power has no effect on the conversion loss after this.

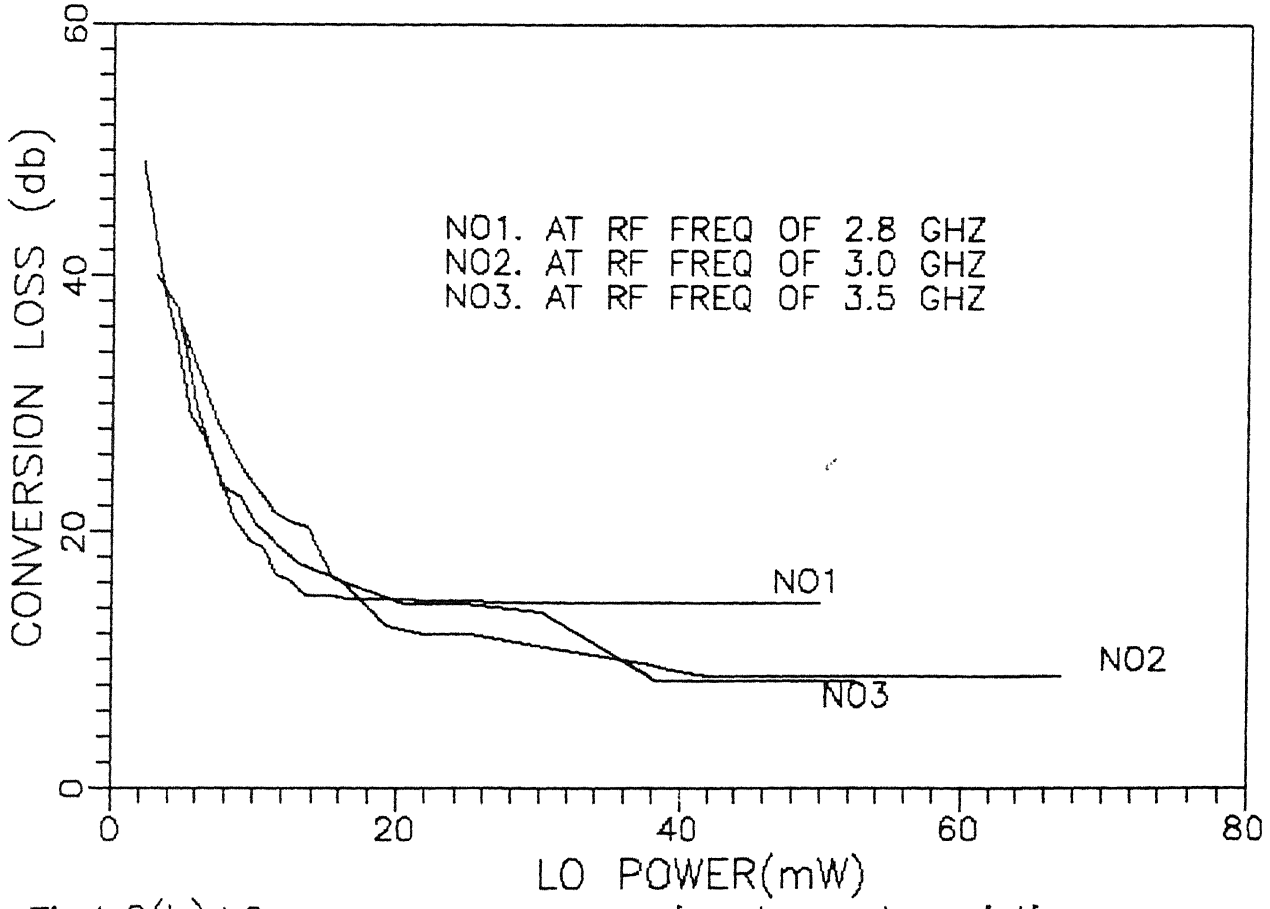

Fig4.6(b) LO power vrs conversion loss chareristic

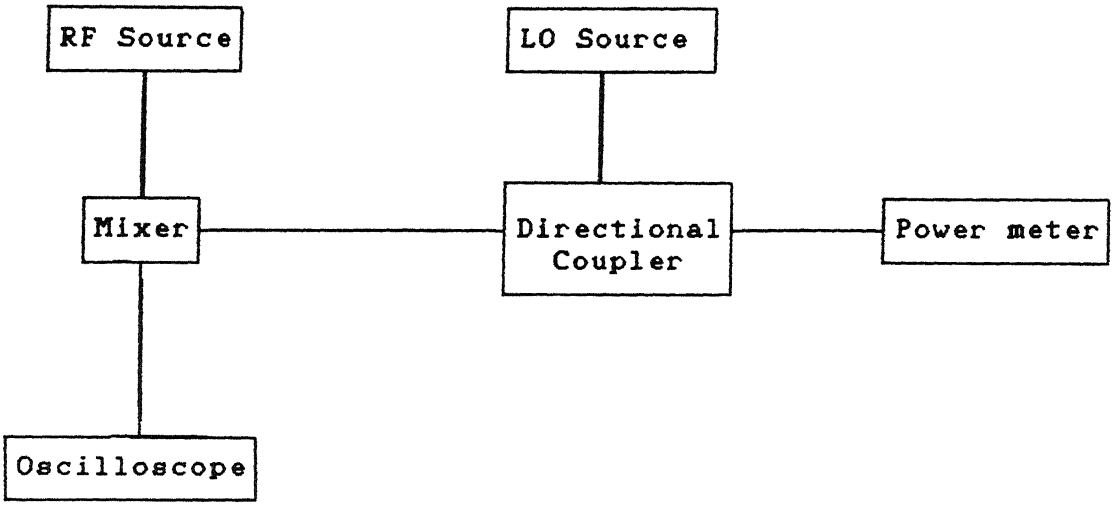

Fig.4.6(a) Experimental set-up for measurement of LO power versus Conversion Loss

4.4.5 Input output characteristics :

The RF signal input and the IF output relations were studied. The 1 dB compression point was also found. The experimental set up for the same is given in fig 4.7 (a).

The input and output relation is shown in fig 4.7 (b). The input and output relation is linear till the saturation point, after which the output does not follow the input. The output is said to be compressed. The 1 dB compression point is specified by the input at which the output drops to 1 dB below projected linear level. This gives input signal range over which the mixer can be used without serious degradation of performance. The lower limit is set by the noise figure and the required signal to noise

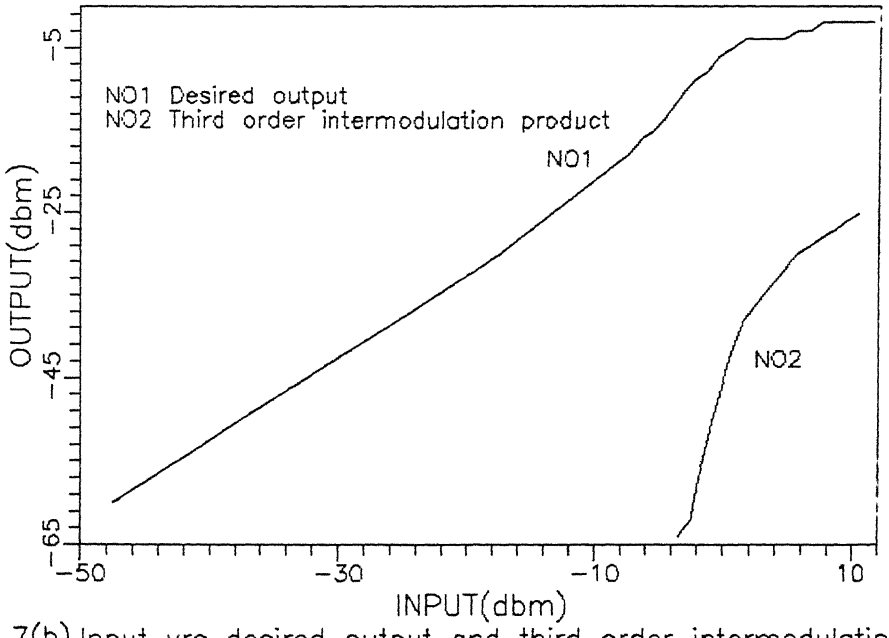

Fig4.7(b) Input vrs desired output and third order intermodulation product

ratio. The upper limit is set by the compression point. The 1 dB compression point was found to be at an input power of +2 dBm and output power level of -5 dBm.

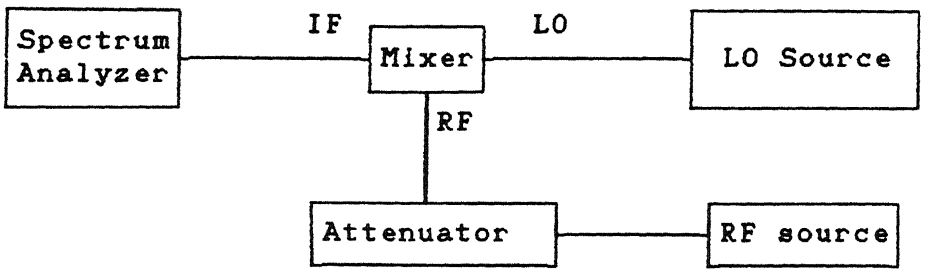

Fig 4.7(a) Measurement set-up for input-output characteristic

4.4.6 Third order intercept point:

When two RF signal f_{s1} and f_{s2} are present at the input, an IF given by $(2f_{s2}-f_{s1}) \pm f_{LO}$ can be generated by the third order term. The theoretical line relating the input to output has a slope of 3, as shown in fig 4.7 (b), compared to the slope of a fundamental line. The third order intercept point is where the fundamental line and the third order line intercepts. The higher the intercept point the better is the third order suppression. This measurement was carried out as shown in fig 4.8. The third order intercept point was found at a input power of +26 dBm and output power of +24 dBm.

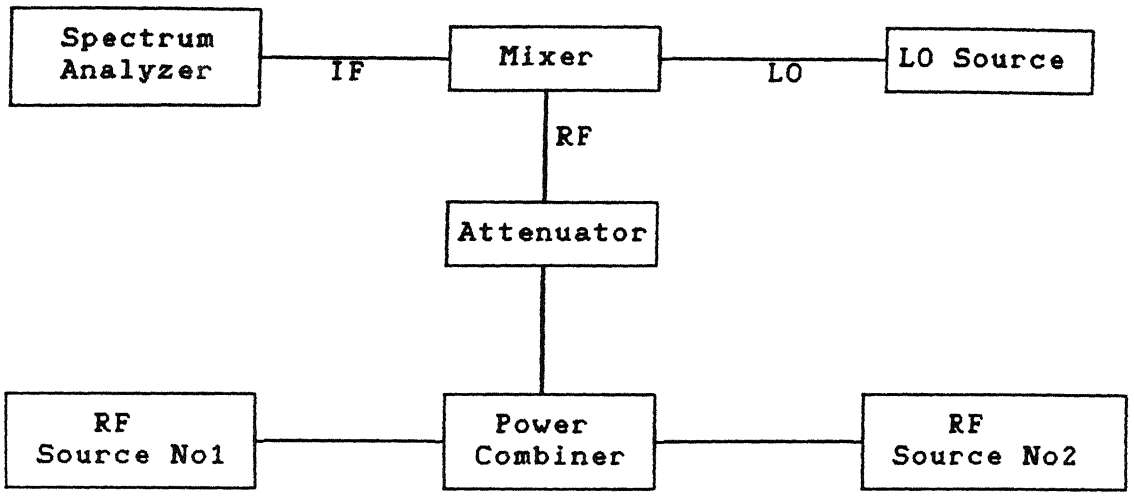

Fig 4.8 Measurement set-up for Third order inter modulation products

4.4.7 Sensitivity Test:

The available input signal level for a given output signal to noise ratio is referred to as the system sensitivity or noise floor. The input voltage level corresponding to this is known as minimum detectable signal. The sensitivity has been expressed in different ways, the most common being tangential sensitivity. This character is subjective, in that its measurement requires some degree of judgment on the part of the person making measurement. To determine the tangential sensitivity, the input power is set at such a value that, the highest peaks in the absence of the signal are at the same level as the lowest noise peaks in the presence of the signal. The input signal level is then the measured tangential sensitivity. It is measured in dBm. The measurement set-up is shown in fig 4.9.

The input RF level is -26 dBm. The attenuation provided to the input is -81 dB. Therefore, the sensitivity of mixer is -107 dBm.

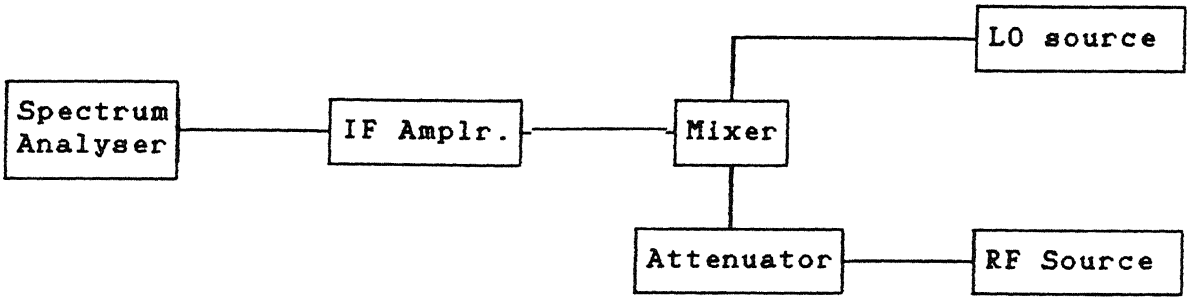

Fig. 4.9 Experimental set up for the sensitivity test of DBM

4.4.8 Isolation between ports :

The isolation between different ports were measured. The isolation as found is given below at a frequency of 3 GHz and LO power level of 10 mW and RF input level at 1 dBm.

Isolation between RF and IF -20 dB

Isolation between LO and IF -40 dB

Isolation between RF and LO -30 dB

4.5 DISCUSSIONS

The work presented in this thesis so far, i.e. the double balanced mixer, was started with a rather ambitious specification of wide band operation over 2GHz to 10GHz. The configuration was arrived at based on the data available on the various transitions,power dividers and the achievable bandwidth of each of these circuits. For example , the reported band width of a

slot line to microstrip transition was from 1 GHz to 10 GHz. However no data was available on the sensitivities of these performance characteristics with respect to the tolerances in the dimensions of the etching patterns. There were also lack of design data for slot line power divider and slot line to microstrip uncoupled junction, which were empirically designed. Another major limitation of the presently fabricated mixer was the diode quad itself , which was optimised for operation up to 3GHz according to manufacturers specification. Higher frequency quads were not available with the department. If a quad designed to work up to 10GHz is used in the same circuit we can expect the Noise Figure and Conversion Loss to be much better than what is reported in this thesis. The mixer fabricated gave reasonably good performance over 2.5 GHz to 4.5GHz. At higher frequencies the diode noise figure itself is higher because the diode are designed for operation up to 3GHz and also the circuit elements seemed to to give larger mismatch losses. The input VSWR was also not within the tolerable limits outside the indicated band of operation.

Some of the causes of poorer performance of the mixer than the designed bandwidth were :

(a) Accuracy of etching- Although this circuit patterns were drawn 1:10 sizes and reduced , the etching was carried out in the usual printed circuit fabrication facility where the etching accuracy was limited. This is specially critical for slot lines whose widths are in 100 to 200μm range.

(b) There was no fixture for accurate alignment of top and

bottom masks , which is very critical for microstrip to slot line transition and uncoupled junction. Two lines, microstrip and slot lines can run parallel on either sides of the substrate with zero coupling only if they are perfectly aligned and centered. Any offset gives rise to coupling between the lines.

(c)The limitations on the physical realization of slot lines of lower impedance, had to be overcome by making compromises on the impedance matching so that higher impedance lines could be made use of.

(d) Presence of several transitions from microstrip to slot lines , junction of CPW and slot/microstrip power divider etc. give rise to some VSWR each which combine to deteriorate the mixer performance. The slot line power divider was empirically designed because it was beyond the scope of the thesis to go into the detailed field analysis of a slot line Tee-junction.

With all these limitations the realized bandwidth was far less than what was aimed at. However, within 2.5GHz to 4.5GHz the performance was found to be satisfactory with noise fig of 5dB and a sensitivity of about -107dBm.

To overcome these limitations of the circuit fabrication , it was decided to try another double balanced mixer configuration which is the subject matter of the next chapter. In this configuration all the transitions from slot line to microstrip were eliminated by the use of a microstrip to symmetrical double strip transmission line. This configuration would not be very sensitive to accuracy of printing and alignment.

CHAPTER 5

DOUBLE BALANCED MIXER -AN ALTERNATE CONFIGURATION

5.1 INTRODUCTION

The broad band DBM which was the aim of this work could not be achieved to satisfaction in the previous configuration due to some design limitations as discussed in chapter 4. Important factors that affected the design were limitation in the accuracy of printing ,alignment of strip and slot line and inadequate design data available for the slot line power divider ,strip slot uncoupled junction and accurate impedance data on even mode of the CPW. It was not possible to go into the in depth theoretical analysis of these within the scope of this thesis work. A new configuration was tried in which some of these drawbacks are eliminated. The transitions between microstrip and slot lines and the power dividers have been eliminated. This configuration is presented in the figure 5.1. The etching pattern is presented in the fig 5.2. This configuration consists of driving the quad by a symmetrical double strip transmission line kept physically orthogonal to achieve isolation between LO and RF signals. The printed circuit consists of a transition from a microstrip transmission line to a symmetrical double strip transmission line. One of this circuit feeds RF and the other feeds LO power. The outputs of these circuits are directly connected to the ring quad. The diode is connected to the top and bottom of the

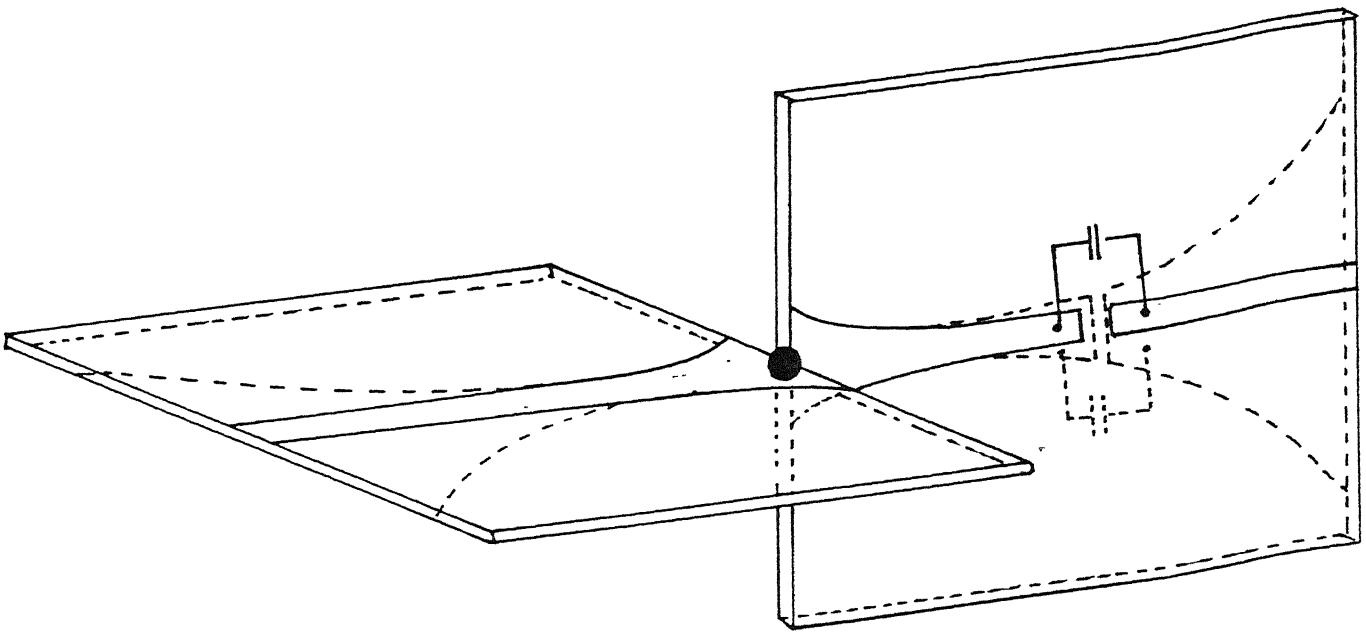

Fig 5.1. circuit configuration of the DBM.

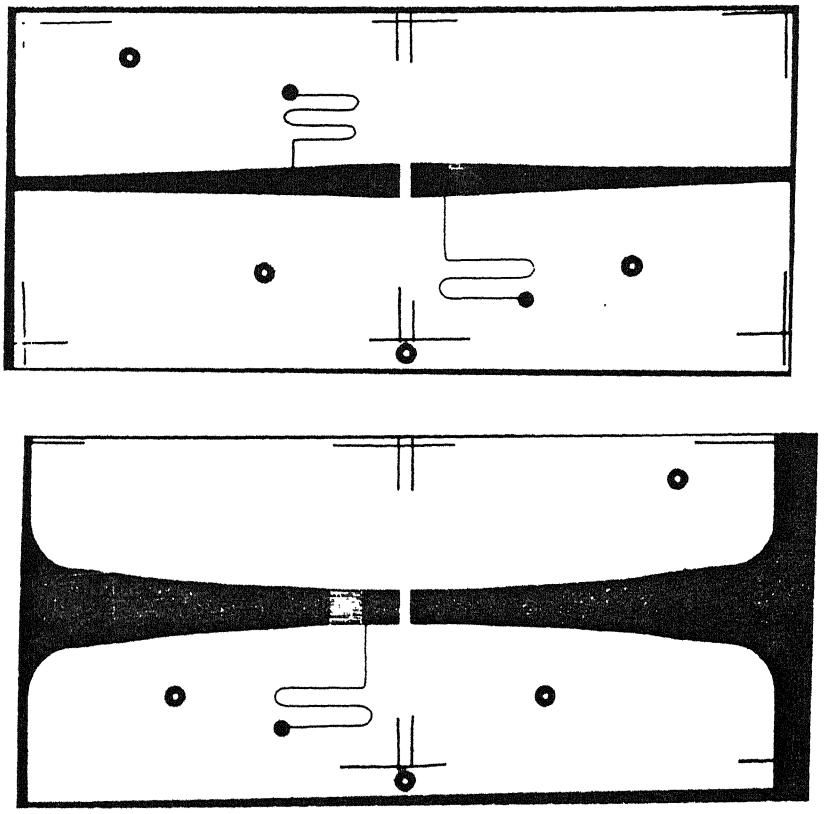

Fig 5.2. Etching pattern for the DBM .

substrate. Therefore, a gap is provided between the two substrates. As the RF and LO circuits are orthogonally placed , their E fields are also orthogonal in space. This provides a better isolation between RF and LO. The IF is obtained from a connection to the microstrip. A fine wire is connected to the microstrip which provides a path for IF. The inductive effect of this long wire gives an isolation of IF from LO and RF. In order to prevent shorting of IF to ground at the lower end of frequency range , DC blocks i.e.series capacitors are provided.

5.2 DESIGN OF A SYMMETRICAL DOUBLE STRIP TRANSMISSION LINE

The main feature in this configuration is the design of symmetrical double strip transmission lines.The RF and LO ports should have an input impedance of 50Ω. For a 10 mW drive the diode quad input impedance is measured to be 20Ω. The present configuration shows two diodes of the ring quad will be in series. Therefore, there is a need for a impedance transformation from 50Ω to 40Ω along with the transition from microstrip to double strip at the diode drive point. Hence these two are combined into one and a microstrip to double strip transition with an impedance transformation ratio of 50/40 is designed. The LO and RF ports have identical transitions. The design procedure can be broadly divided into:

(a) Design of microstrip to double strip transition

(b) Design of taper for impedance matching.

5.2.1 Design considerations of a double strip transmission line

The mixer as shown in fig 5.1 uses a very simple balun

structure to realize a transition from a microstrip to symmetrical double strip transmission line. The ground plane conductor is much wider than the top conductor at the input end. Gradually the wider ground plane is tapered to the width of the microstrip conductor width. The symmetrical double strip transmission line is shown in fig 5.3(a). It consists of two conductors of same width w on opposite faces of the substrate. As the field lines are symmetric about the center height of the substrate as shown in fig 5.3 (a) ,an electric wall can be placed along the layer. This will resemble like a thin metal plate of infinity conductivity. This of course will not disturb the electric and magnetic field lines. Therefore, the double strip transmission line can be represented as two microstrip lines with same conductor width but half the substrate thickness. This is shown in fig 5.3 (b). Therefore, the circuit parameters, characteristic impedance Z_{ds} and effective permittivity ε_{reffds} of a double strip transmission line(w,h,ε_r) can be derived from Z_{dm}, ε_{reffm} of a microstrip line with the same conductor width w and half the substrate thickness h as a substrate with the same ε_r.

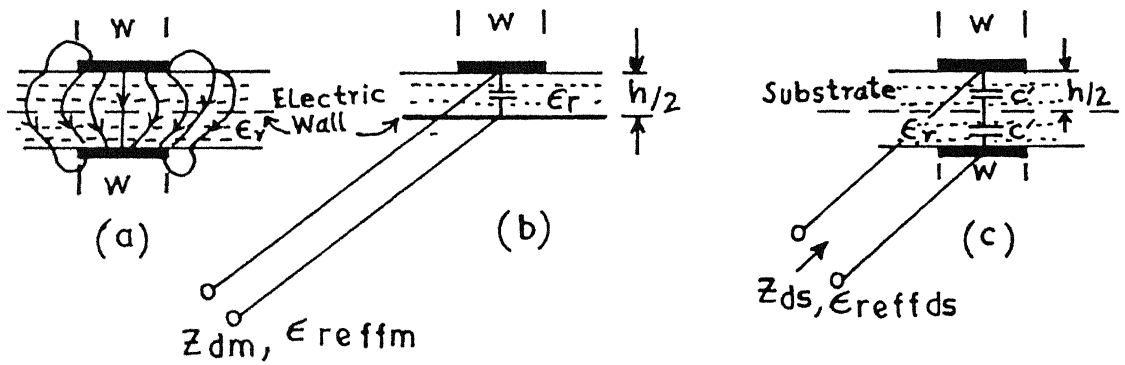

Fig 5.3 Symmetrical Double strip transmission line

5.2.2 Design considerations of taper for impedance transformation

R. W. Klopfenstein [13] reported about the transmission line taper of improved design. The theory of design of optimal cascaded transformer arrangements are extended to the design of continuous transmission line tapers. The performance of the Dolph-Tchebycheff transmission line taper has a minimum reflection coefficient magnitude in the pass band for a specified length of taper , similarly , for a specified maximum magnitude reflection coefficient in the pass band , the Dolph-Tchebycheff taper has minimum length. Therefore, this design is adopted for the transformer.

In the present work , the impedance transformation taper is included along with the transition from microstrip to symmetrical double strip transmission line.

5.3 DESIGN OF TRANSITION AND IMPEDANCE TRANSFORMER.

The fabrication of the circuit is done on a duroid substrate with ε_r of 10.5 and h of 1.587 mm.

(a) Design of taper:

As already discussed earlier the design of an optimal 50Ω to 40Ω microstrip to double strip transmission line in such a way that the reflection coefficient magnitude does not exceed about 1% in the pass band.

$$\rho_o = 0.5 \ln \frac{Z_2}{Z_1}$$

$$\rho_o = 0.5 \ln \frac{50}{40} = 0.111$$

The VSWR corresponding to this is 1.24

It is required that the maximum reflection coefficient magnitude in the pass band should not exceed 0.1 of the ρ_o. Accordingly the VSWR is 1.02. The reflection coefficient magnitude takes on it's maximum value $|\rho_o|$ at zero frequency and oscillates in the pass band constant amplitude equal to $\rho_o/\cosh A$

Therefore,

$$\frac{\rho_o}{\cosh A} = \frac{\rho_o}{10}$$

Therefore, A = 3.0

The specification of the parameter A determines the maximum magnitude of reflection coefficient in the pass band. The pass band consists of all frequencies such that $\beta l >= A$.

If $\beta l = A$, then $\frac{l}{\lambda_g} = \frac{A}{2\pi} = 0.47746$

We assume the lower cutoff frequency as 2 GHz. Therefore, calculated λ_g=5.76Cmand λ_g=5.06Cm. Hence l = λ_g*0.47746=2.75016cm or l=2.39016cm. Assumed length for the design is 30 mm Length considered in the design is more than the maximum length. Referring [13] the characteristic impedance at different sections are found out. The total length of 30 mm is equally divided into 10 sections. At each section the tapered impedances are calculated. These are shown in table No 1.

(b) Design of transition from microstrip to double strip

The design details of a transition from a microstrip to

TABLE NO. 1

DESIGN DATA OF TRANSITIONS BETWEEN MICROSTRIP TO DOUBLE STRIP LINE.

Distance from microstrip end in mm	width of microstrip (W_1) in mm	Characteristic Impedance (Z_o) in ohms	Ratio W_2/W_1 (x)	Width of ground plane (W_2) in mm
0	1.476	50	5	6
3	1.730	47.7	4.5	3.5955
6	1.8735	47.2	3.75	3.243
9	2.0285	46.6	3	2.81
12	2.1964	46	2.4	2.4342
15	2.1964	45.3	2.05	2.2513
18	2.3781	44.7	1.65	1.961
21	2.574	43.4	1.55	1.96
24	2.788	42.8	1.3	1.81
27	3.018	42.3	1.05	1.584
30	3.2685	40	1	1.634

symmetrical double strip are not available in the literature.The impedance data for micro strip and double strip lines are available. The transformer is required to provide a smooth transition of transmission line from microstrip to double strip. Some empirical assumptions were made to interpolate the microstrip and double strip impedance data,to derive an empirical formula for the transition region where the line has two strips of different width. The transition length is taken to be longer than optimum Klopfenstein taper length , to make the design less sensitive to small errors in the characteristic impedance of the lines of transition region. This uses empirically derived formula. A transition calculation has been carried out assuming the transmission line having effect of both microstrip and double strip. Firstly the microstrip and double strip characteristics are plotted in terms of their characteristic impedance and ratio of width of the conductor to the thickness of the substrate. The width of the ground plane is assumed as W_2 and width of top conductor as W_1 With characteristic impedance of 50Ω the microstrip end width is found to be 1.476 mm referring [6]. The double strip end having an impedance of 40Ω the width is equal to 3.27mm. The microstrip conductor width (W_1) variation was assumed to be exponential. Width at ten equal sections were found out. this is presented in the table No1. The characteristic impedance vs W_1/h was calculated at other points by assuming a function f(x). The function f(x) assumed is $(x)^{-n}$ where x is the ratio of W_2 to W_1 and the impedance is calculated as:

$$Z_o=[Z_{ds}* f(x)+Z_{ms}* (1- f(x))] .$$

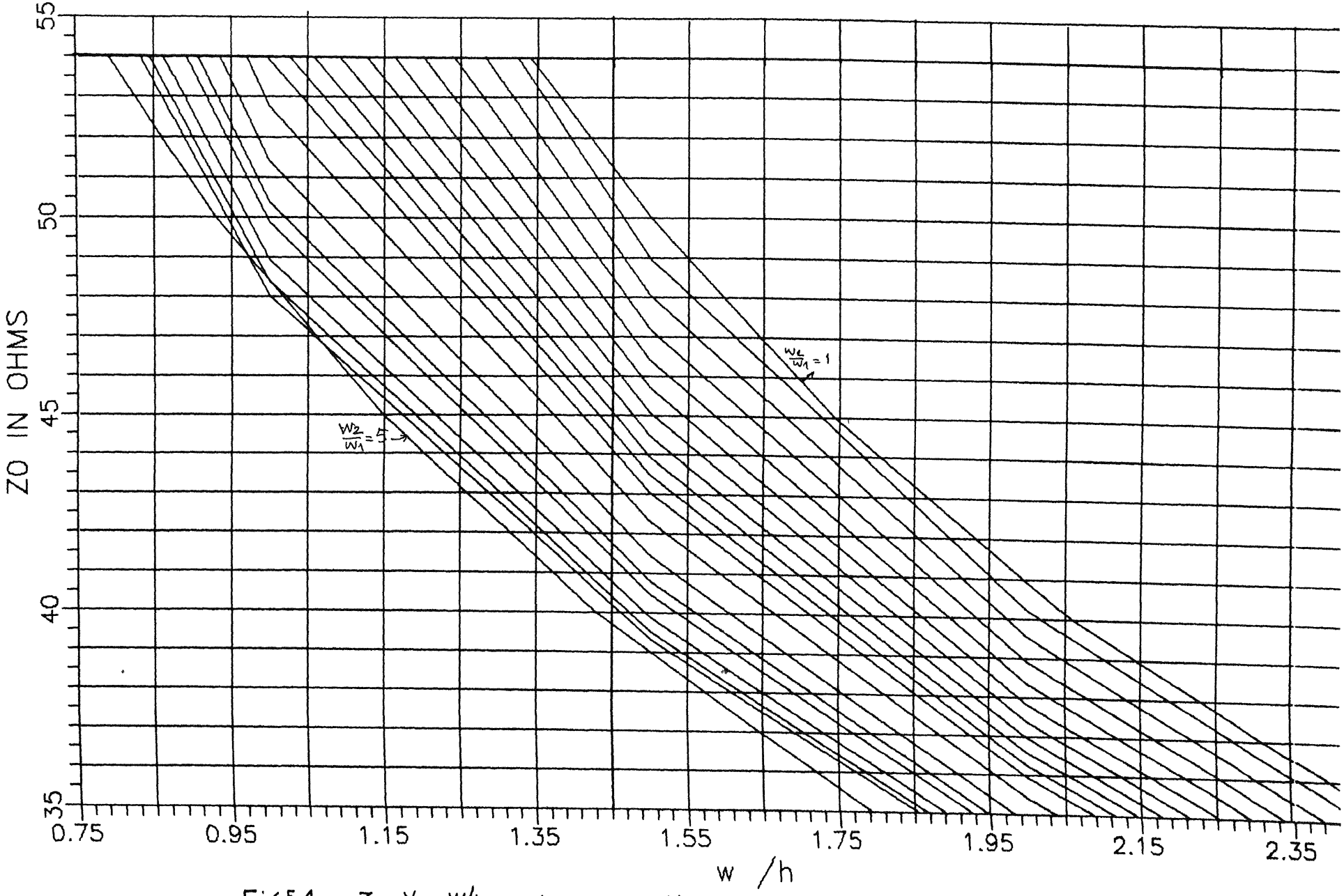

Fig 5.4 Z_o Vs W/h characteristic of the transition

A computer program is prepared to give the characteristic impedance of combined double strip and microstrip at different W_1/h locations. These characteristics are plotted in fig 5.4. Having the plots, the design of the transition is found easier. The characteristic impedance of the sections are calculated from taper formula. W_1 is already been assumed as having an exponential characteristics. Therefore, from the plot, the intersection points gives the value of W_2/W_1. Thus W_2 value is determined. Table 1 gives the details of the location from the microstrip end the values of W_1 , W_2/W_1 and value of W_2.

5.4 PERFORMANCE CHARACTERISTIC

5.4.1 Reflection Coefficient at RF and LO ports:

Reflection coefficient measured at RF port at different frequencies are shown in fig 5.5. The reflection coefficient magnitude was found to be within -10dB between 2 GHz and 3.5 GHz. At 3.5 GHz and 5 GHz the reflection coefficient is found to be high. This may be due to resonance at that particular frequencies.

The LO port reflection coefficient is shown in fig 5.6 at different frequencies. The reflection coefficient magnitude was found to be within 0.3 from a frequency of 2.5 GHz up to 4 GHz. From 4 GHz up to 5.5 GHz there is a gradual increase. However, the reflection coefficient was varying after 5.5 GHz. This is due to mismatches in the circuit parameters.

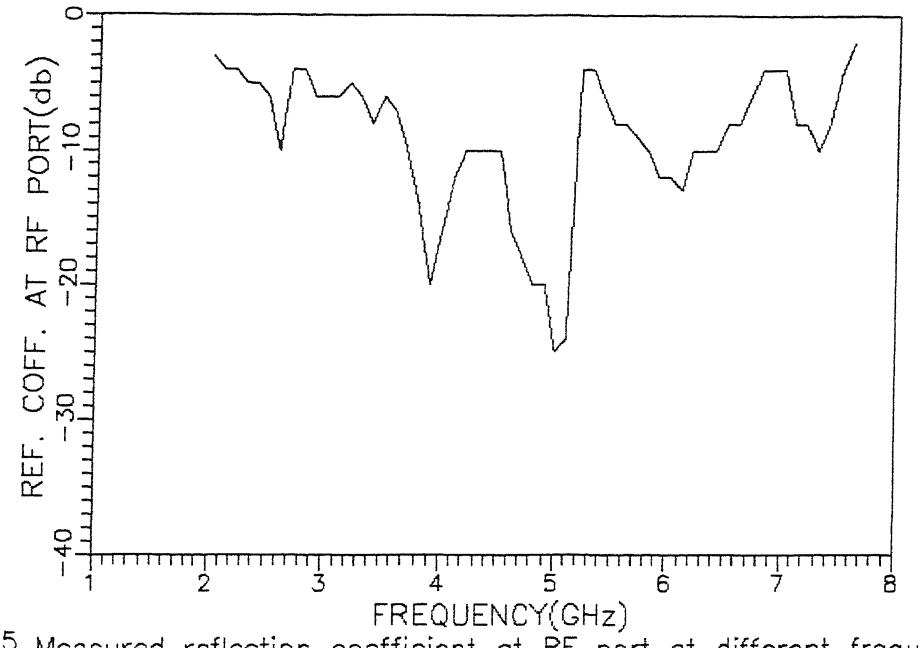

Fig 5.5 Measured reflection coefficient at RF port at different frequencies

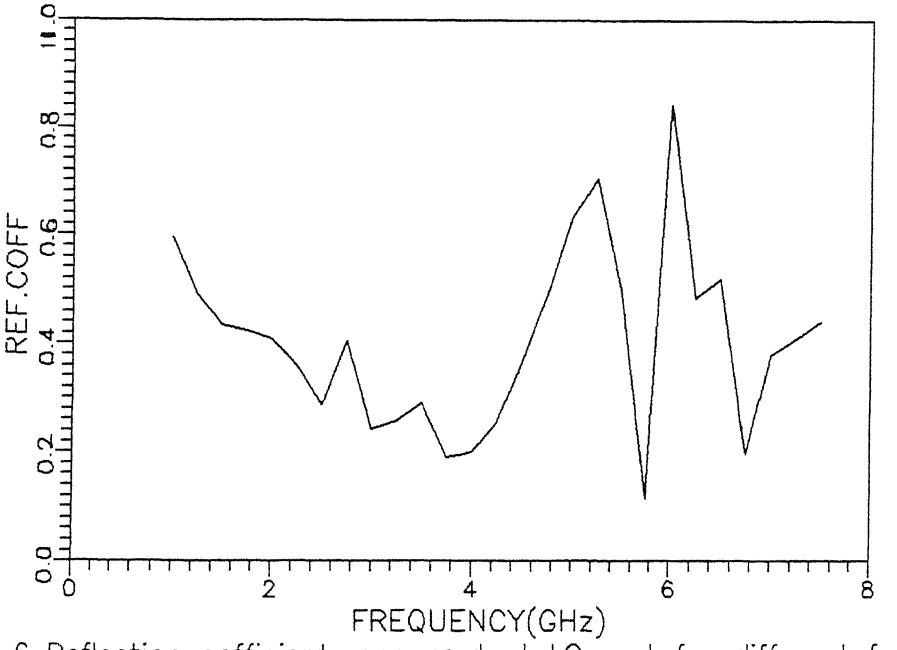

Fig5.6 Reflection cofficient measured at LO port for different frequencies

5.4.2 Conversion loss characteristics :

The measured conversion loss in dB has been plotted at different frequencies in fig 5.7. The conversion loss was found to be within 6 dB from 2 GHz to 5 GHz. In the frequency range of 5 GHz to 6.5 GHz, the conversion loss was found to be within 8 dB. There is sharp increase of conversion loss after this frequency. The increase of conversion loss is mainly due to the quad parasitic elements. Quad is optimized for operation up to 3 GHz and above this frequency there is a gradual increase in the conversion loss.

5.4.3 Noise Figure Characteristics :

The noise figure of the mixer was measured at different frequencies. This is shown in fig 5.8. The measured noise figure was below 5 dB from 2 GHz to 3 GHz. From 3 GHz to 5 GHz the noise figure was within 10 dB. From 5 GHz to 7 GHz the noise figure was found to increase up to 11 dB. After 3 GHz the noise figure is high mainly due to noise figure of the diode quad above 3 GHz and also due to mismatches in the circuit.

5.4.4 Local Oscillator Power Vs Conversion Loss :

The effect of LO power on the conversion loss is measured at three different RF frequencies. The characteristics are presented in fig 5.9. It is observed that below 10 mW of LO power the conversion loss increases. It levels down from LO power of 10 mW and remains almost constant after about 20 mW of LO power. There is no effect in conversion loss after 20 mW of

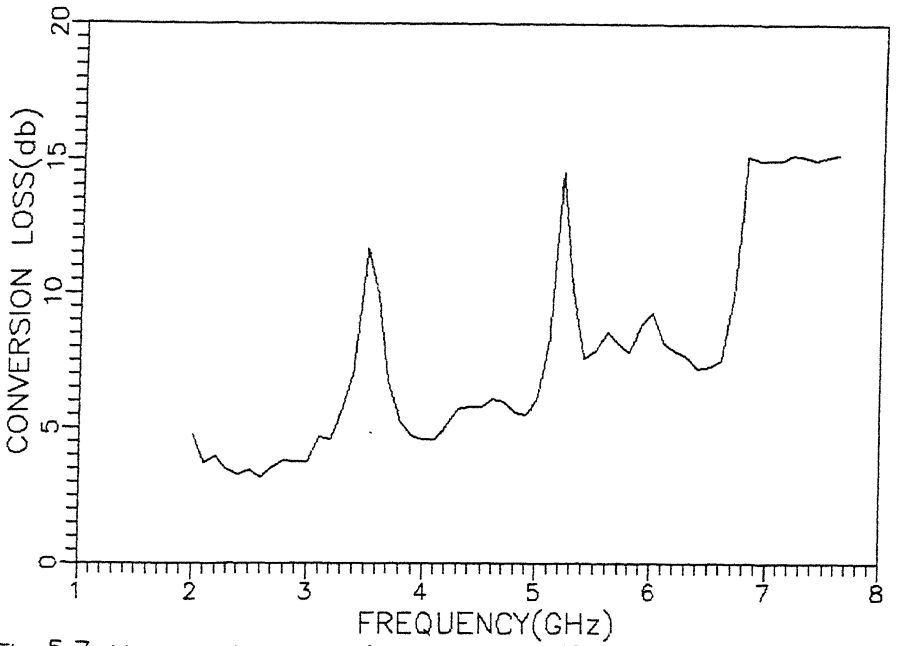

Fig 5.7 Measured conversion loss at different frequencies

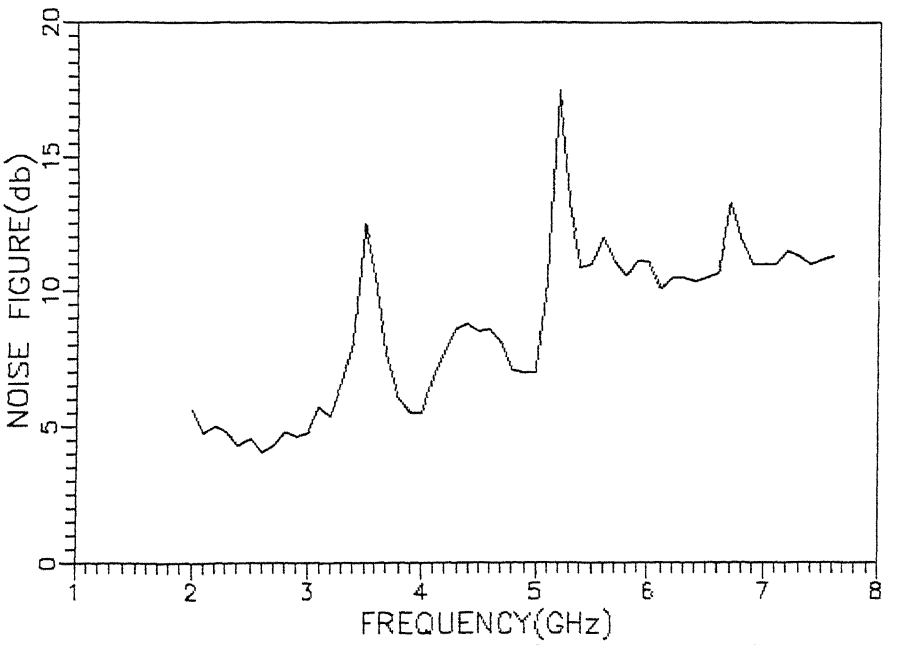

Fig 5.8 Measured noise figure at different frequencies

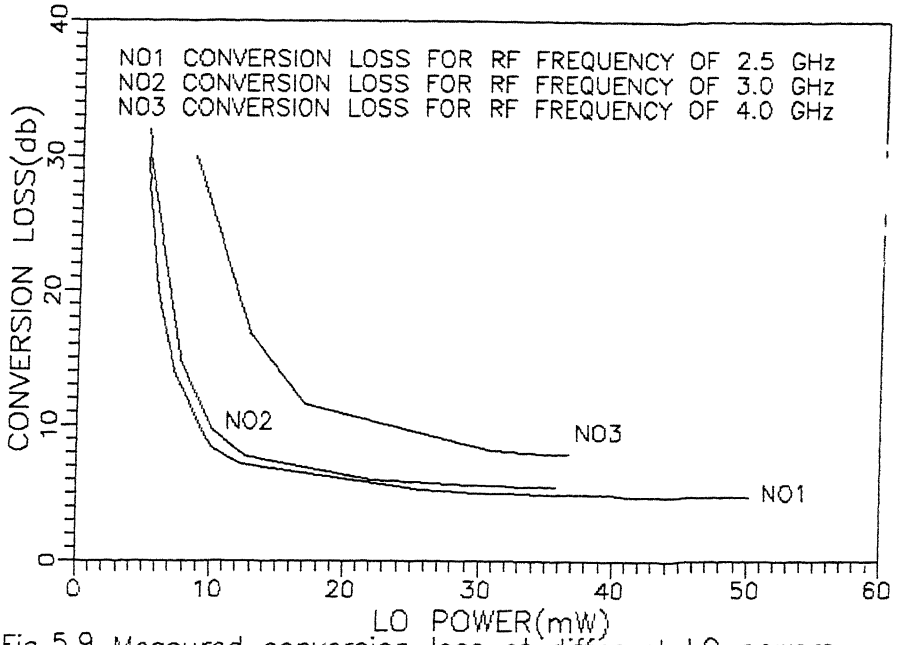

Fig 5.9 Measured conversion loss at different LO powers

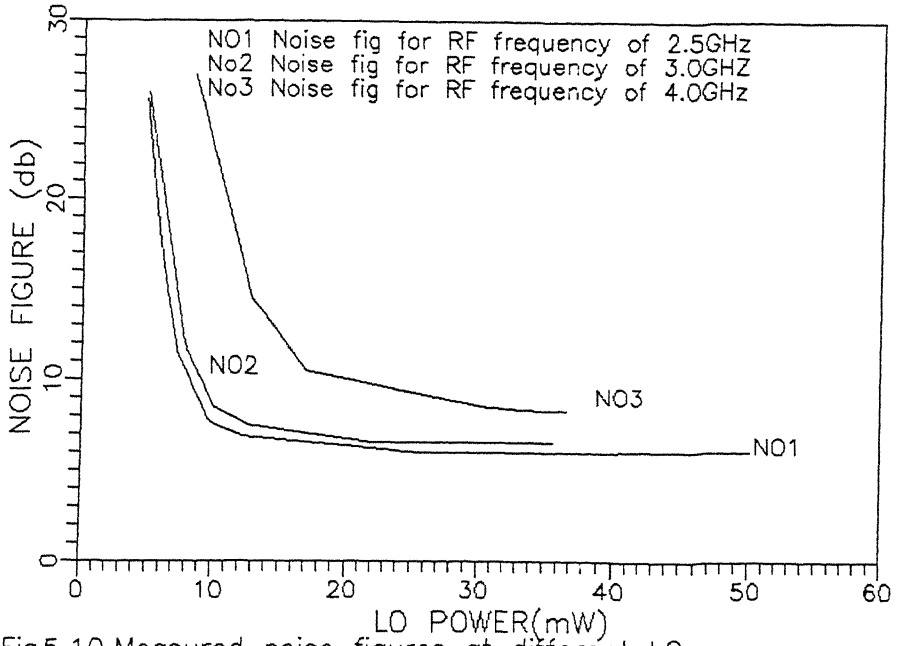

Fig5.10 Measured noise figures at different LO powers

LO power.

5.4.5 Local Oscillator Power Vs Noise Figure :

The effect of LO power on the noise figure is shown in fig 5.10. It is observed that below 10 mW of LO power the noise figure increases. It levels down from LO power of 15 mW and remains almost constant after 20 mW of LO power.

5.4.6 Input Output Characteristics and Third Order Intercept Point :

The input output characteristics along with third order inter modulation product is presented in fig 5.11. It is observed that the 1 dB compression point is at an input level of +6dBm and output level of -7dBm. The third order intercept point is at an input of +40 dBm and output level of +26 dBm.

5.4.7 Sensitivity and Port Isolation Characteristics :

The sensitivity was measured to be -104 dBm at a noise figure level of 4.75 dB.

Isolation between different ports are measured at a frequency of 3 GHz and LO power level of 10 mW. The isolation between ports are given below.

Isolation between RF and IF port is -26 dB.

Isolation between LO and IF port is-20 dB.

Isolation between LO and RF port is-35 dB.

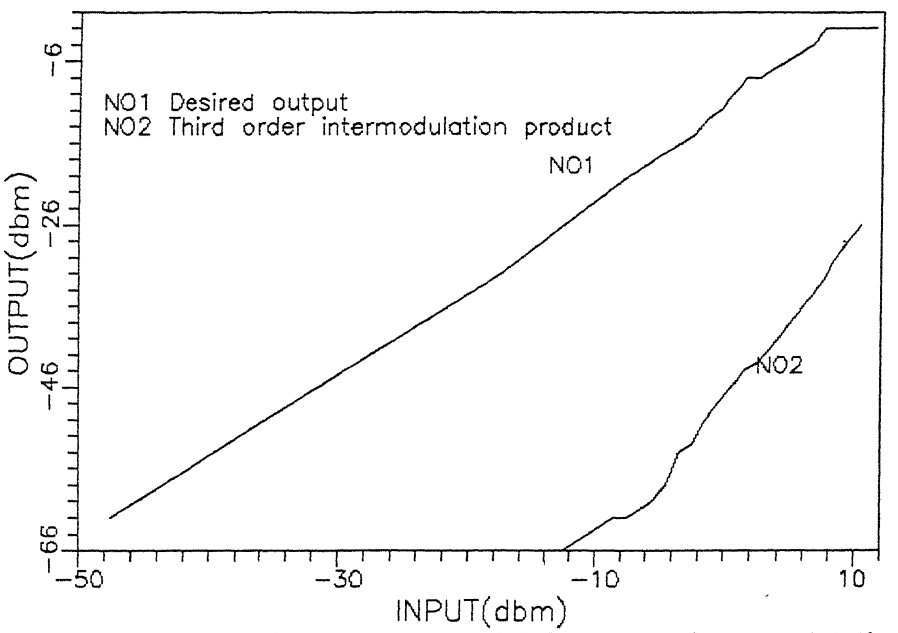

Fig5.11Input vrs desired output and third order intermodulation product

5.5 CONCLUSION

This configuration was adopted mainly to improve upon the results obtained from the previous configuration. This design configuration primarily consists of transition from microstrip to double strip transmission line with impedance transformation. The design details of the transition from a microstrip line to double strip line were not available. Therefore, an empirical formula was derived for transition region. The printing accuracy was not a major criteria in this configuration. A trial for printing of interdigital capacitors on the same substrate was done. But the fine etching could not be realized. Therefore Chip capacitors are used in it's place. The mixer performed better in the frequency range of 2GHz to 4.5GHz with noise figure within 6dB and Conversion loss within 6dB. The performance of this mixer was satisfactory from 4.5GHz to 6.5GHz with a noise figure within 10dB and conversion loss of 7.5dB. The high noise figure at the higher frequency is mainly due to the diode quad which is optimized for operation up to 3GHz. It is also found that at some frequencies the circuit mismatch was high. This may be due to resonances at these frequencies. The isolation between the ports are found to be better. The RF and LO port isolation of -35 dB , RF and IF isolation of -26 dB were measured. This circuit performance was found to be superior to the previous circuit configuration.

CHAPTER 6

CONCLUSION

The design and performance characteristics of the two double balanced mixers configurations were considered keeping in view the broad band operation. The first configuration did not give satisfactory results. The reasons are nonprecision printing techniques, inadequate design data. In the course of this work, it was found that no study has been carried out on uncoupled junction between microstrip and slot lines. These were experimentally optimized for lowest coupling. The CPW even mode impedance data are inadequate for proper design. The slot line power divider design data was also not available. Some approximate design has been used for this.

The second configuration was adopted mainly to improve upon the results of the previous configuration. The drawbacks of the first design are eliminated in the second configuration. The second DBM circuit consists of a transition from microstrip to symmetrical double strip transmission line with impedance transformation. The RF and LO circuits are orthogonally placed to provide better isolation between RF and LO. The impedance transformation design is adopted mainly from the works of Klopfenstein. The design data for transition from microstrip to double strip was not available. Therefore, an empirical formula was formulated to design the transition. It was beyond the scope

of the thesis to go into the detail field analysis of the transition.

The mixer performed better in the frequency band of 2GHz to 6.5GHz. The overall noise figure was below 6dB and conversion loss within 6dB from 2GHz to 4.5GHz. Even from 4.5 GHz to up to 6.5GHz, the conversion loss was within 7.5dB. The noise figure was 10db in this range of frequencies,because the noise figure performance of the diode quad limits the noise figure of the mixer. It was found that at some frequencies the circuit mismatch was high. This may be due to resonances at these frequencies. The isolation between LO and RF ports is found to be -35dB.Therefore,the second circuit performance is found to be suitable for a broad band operation.

REFERENCES

1. H.C.Torrey and C.A.Whitmer, Crystal Rectifiers, MIT radiation lab. Series, Vol.15, New Work : McGraw-Hill, 1948.

2. L.E.Dickens and D.W.Maki, "An integrated-circuit balanced mixer, image and sum enhanced ", IEEE Trans. Microwave Theory Tech., Vol. MTT-23, Mar 1975.

3. G.Begemann, "An X-band balanced fin line mixer", IEEE Trans. Microwave Theory Tech., Vol. MTT-26, Dec 1978 .

4. M.V.Schneider and W.W.Snell, "Harmonically pumped stripline down converter", IEEE Trans.Microwave Theory Tech., Vol.MTT-23, Mar 1975.

5. Hiroyo Ogawa, Masayoshi Aikawa and Kozo Morita, "K-Band Integrated Double Balanced Mixer", IEEE Trans.Microwave Theory Tech., Vol. MTT-28 March 1980.

6. R.K.Hoffmann, Hand book of Microwave integrated Circuits,Artech House , 1987 .

7. K.C.Gupta, et al., Microstrip lines and Slot lines, Artech House, 1979.

8. B.Schiek and J.K.Ohler, "An improved Microstrip to Microslot Transition ", IEEE Trans. Microwave Theory Tech., Vol. MTT-24, 1976.

9. Edward T C,Foundations for Microstrip design ,John Wiley and Sons, 1981.

10. Jack Smith, Modern communication circuits , McGraw Hill 1986.

11. H.P.Walker, "Sources of Intermodulation in diode-ring Mixers ",The Radio and Electronic Engineer , Vol 46, No 5 , May 1976.

12. Bernd Schuppert, "Analysis and Design of Microwave Balanced Mixers" IEEE Trans. Microwave Theory Tech., Vol. MTT-34. No1, Jan 1986.

13. R W Klopfenstein, " A Transmission line taper of Improved Design ", Proceedings of IRE , Jan 1956.

14. Wilkinson E , "An N-Way Hybrid Power divider", IEEE Trans. Microwave Theory Tech., Vol. MTT-8, Jan 1960.

15. Cohn S.B , " A class of Broad band 3-port TEM hybrids ", IEEE Trans. Microwave Theory Tech., Vol. MTT-16 , Feb 1968.

16. Krauss Bostian Rabb, Solid state Radio engineering, John Wiley and Sons 1980.

17. Davis, Microwave Semiconductor circuit Design, Van Nostrand rein hold company, Newyork, 1984.

18. Bahl and Bhartia, Microwave Solid state circuit Design ,John Wiley and Sons, 1988.

19. S A Mass, Microwave Mixers, Artech house, 1986.

20. Pound,Microwave Mixers, Radiation laboratory series MIT, cambridge, 1948.